

Off-line approximate dynamic programming for the vehicle routing problem with a highly variable customer basis and stochastic demands

M. Dastpak, F. Errico, O. Jabali

G-2021-53

September 2021

Revised: Juin 2022

La collection *Les Cahiers du GERAD* est constituée des travaux de recherche menés par nos membres. La plupart de ces documents de travail a été soumis à des revues avec comité de révision. Lorsqu'un document est accepté et publié, le pdf original est retiré si c'est nécessaire et un lien vers l'article publié est ajouté.

Citation suggérée : M. Dastpak, F. Errico, O. Jabali (Septembre 2021). Off-line approximate dynamic programming for the vehicle routing problem with a highly variable customer basis and stochastic demands, Rapport technique, Les Cahiers du GERAD G- 2021-53, GERAD, HEC Montréal, Canada.

Avant de citer ce rapport technique, veuillez visiter notre site Web (<https://www.gerad.ca/fr/papers/G-2021-53>) afin de mettre à jour vos données de référence, s'il a été publié dans une revue scientifique.

La publication de ces rapports de recherche est rendue possible grâce au soutien de HEC Montréal, Polytechnique Montréal, Université McGill, Université du Québec à Montréal, ainsi que du Fonds de recherche du Québec – Nature et technologies.

Dépôt légal – Bibliothèque et Archives nationales du Québec, 2021
– Bibliothèque et Archives Canada, 2021

The series *Les Cahiers du GERAD* consists of working papers carried out by our members. Most of these pre-prints have been submitted to peer-reviewed journals. When accepted and published, if necessary, the original pdf is removed and a link to the published article is added.

Suggested citation: M. Dastpak, F. Errico, O. Jabali (September 2021). Off-line approximate dynamic programming for the vehicle routing problem with a highly variable customer basis and stochastic demands, Technical report, Les Cahiers du GERAD G-2021-53, GERAD, HEC Montréal, Canada.

Before citing this technical report, please visit our website (<https://www.gerad.ca/en/papers/G-2021-53>) to update your reference data, if it has been published in a scientific journal.

The support of these research reports is made possible thanks to the support of HEC Montréal, Polytechnique Montréal, McGill University, Université du Québec à Montréal, as well as the Fonds de recherche du Québec – Nature et technologies.

Legal deposit – Bibliothèque et Archives nationales du Québec, 2021
– Library and Archives Canada, 2021

Off-line approximate dynamic programming for the vehicle routing problem with a highly variable customer basis and stochastic demands

Mohsen Dastpak ^{a, b, c}

Fausto Errico ^{a, b, c}

Ola Jabali ^d

^a *Department de génie de la construction, École de technologie supérieure, Montréal (Qc), Canada, H3C 1K3*

^b *GERAD, Montréal (Qc), Canada, H3T 1J4*

^c *CIRRELT, Montréal (QC), Canada, H3C 3J7*

^d *Dipartimento di Elettronica, Informazione e Bioingegneria, Politecnico di Milano, Piazza Leonardo da Vinci 32, Milano 20133, Italy*

mohsen.dastpak.1@ens.etsmtl.ca

fausto.errico@cirrelt.ca

ola.jabali@ens.etsmtl.ca

September 2021

Juin 2022

Les Cahiers du GERAD

G–2021–53

Copyright © 2021 GERAD, Dastpak, Errico, Jabali

Les textes publiés dans la série des rapports de recherche *Les Cahiers du GERAD* n'engagent que la responsabilité de leurs auteurs. Les auteurs conservent leur droit d'auteur et leurs droits moraux sur leurs publications et les utilisateurs s'engagent à reconnaître et respecter les exigences légales associées à ces droits. Ainsi, les utilisateurs:

- Peuvent télécharger et imprimer une copie de toute publication du portail public aux fins d'étude ou de recherche privée;
- Ne peuvent pas distribuer le matériel ou l'utiliser pour une activité à but lucratif ou pour un gain commercial;
- Peuvent distribuer gratuitement l'URL identifiant la publication.

Si vous pensez que ce document enfreint le droit d'auteur, contactez-nous en fournissant des détails. Nous supprimerons immédiatement l'accès au travail et enquêterons sur votre demande.

The authors are exclusively responsible for the content of their research papers published in the series *Les Cahiers du GERAD*. Copyright and moral rights for the publications are retained by the authors and the users must commit themselves to recognize and abide the legal requirements associated with these rights. Thus, users:

- May download and print one copy of any publication from the public portal for the purpose of private study or research;
- May not further distribute the material or use it for any profit-making activity or commercial gain;
- May freely distribute the URL identifying the publication.

If you believe that this document breaches copyright please contact us providing details, and we will remove access to the work immediately and investigate your claim.

Abstract : We study a stochastic variant of the vehicle routing problem (VRP) arising in the context of domestic donor collection services. The problem we consider combines the following attributes. Customers requesting services are *variable*, in the sense that the customers are stochastic, but are not restricted to a predefined set, as they may appear anywhere in a given service area. Furthermore, demand volumes are also stochastic and are observed upon visiting the customer. The objective is to maximize the expected served demands while meeting vehicle capacity and time restrictions. We call this problem the VRP with a highly Variable Customer basis and Stochastic Demands (VRP-VCSD). For this problem, we first propose a Markov Decision Process (MDP) formulation representing the classical *centralized* decision-making perspective where one decision-maker establishes the routes of all vehicles. While the resulting formulation turns out to be intractable, it provides us with the ground to develop a new MDP formulation, which we call *partially decentralized*. In this formulation, the action-space is decomposed by vehicle. However, the decentralization is not complete as we enforce identical vehicle-specific policies, while optimizing the collective reward. We propose a number of strategies to reduce the dimension of the state and action spaces associated with the partially decentralized formulation. These yield a considerably more tractable problem, which we solve via Reinforcement Learning. In particular, we develop a Q-learning algorithm called DecQN, which features state-of-the-art acceleration techniques such as Replay Memory and Double Q Network . We conduct a thorough computational analysis. Results show that DecQN considerably outperforms three benchmark policies. Moreover, when comparing with existing literature, we show that our approach can compete with specialized methods developed for the particular case of the VRP-VCSD where customer locations and expected demands are known in advance. Finally, we show that the value functions and policies obtained by DecQN can be easily embedded in Rollout algorithms, thus further improving the performances of DecQN.

Keywords: Stochastic Vehicle Routing Problem, Approximate Dynamic Programming, Q-learning, Decentralized Decision-Making

1 Introduction

More than two billion tonnes of municipal solid waste (MSW) is annually generated. This figure is expected to increase by 70% by 2050 (Kaza et al. 2018). The importance of globally containing and diminishing waste has been receiving increasing attention from policymakers. For example, waste reduction is key in several targets of the UN Sustainable Development Goals, notably target 12.5 states that “by 2030, substantially reduce waste generation through prevention, reduction, recycling and reuse” (UN 2021). This target is to be measured by national recycling rates. Recycling has also been central to EU policies. According to the 2020 EU circular economy action plan, member states must recycle or prepare for reuse at least 60% of their municipal waste by 2030 (EEA 2022). Alongside the efforts invested in promoting recycling, policymakers are also exploring means of avoiding waste altogether.

Several initiatives targeting waste prevention fall under the broad title of circular economy (CE). For a comprehensive overview of the research on waste management within CE, we refer the reader to Ranjbari et al. (2021). Within this context, we focus our attention on applications related to product reuse and the rise of online platforms to facilitate it. We then discuss a specific transportation problem arising in such platforms.

Reuse entails extending product life cycle by having the product (or its materials) used by people that are different from its original owners (Fortuna and Diyamandoglu 2017). One of the most studied applications of product reuse relates to textile and fashion items. As noted by Shirvanimoghaddam et al. (2020), the disposal nature of *fast fashion* coupled with the throwaway culture is resulting in serious environmental, social and economic problems. Indeed, fast fashion firms may be legally forced to collect more preowned items for reuse and recycling (Zanjirani Farahani, Asgari, and Van Wassenhove 2021). For a comprehensive review of the environmental impact resulting from textile reuse and recycling, we refer the reader to Sandin and Peters (2018). Although less studied in the literature, another important application of product reuse relates to furniture. According to the EPA, 12.2 million tons of furniture waste generated in 2017, with 80.2% of it ending up in landfills (US EPA 2019). Curran and Williams (2010) analyzed the operations of nearly 400 furniture reuse organizations (FROs) in England and Wales. The term FRO reflects the primary type of household item dealt with, yet other types of items are now commonly collected, including electrical appliances and IT equipment. The study indicates that donors often only have to wait one or two days for the collection of their items.

A number of digital-based platforms have been developed to support household-based MSW reduction and CE principles. Gu et al. (2019) study the environmental performance of MSW recycling associated with Aibolv, a WeChat applet. This mobile application allows individual users to place requests of disposing their MSW; then nearby operators are matched and dispatched to collect it. A wide variety of MSWs are considered, including kitchen tools and spent textiles. Rosu et al. (2017) propose the Social Needs Marketplace, which is a platform for the efficient and effective provisioning of goods for vulnerable populations. The aim of the platform is to provide an efficient way to redistribute goods by directly matching individual donors and volunteer transporters with recipients. Considering the use case of furniture donations, the platform addresses logistical problems such as scheduling collection services using a volunteer network.

In this paper, we study a distribution planning problem arising in the context of Domestic Donor Collection Services (DDCSs). Inspired by platforms such as Big Brothers Big Sisters (2022) and 211 of Greater Montréal (2022), which deploy DDCSs, we identify a number of unique modeling characteristics. First, similar to e-commerce applications, DDCSs deal with a very large basin of service requests, potentially comprising all residential addresses in a city. The number of customers to be served each day is, however, limited and generally highly variable from one day to another. Second, DDCSs require donors to classify the size of their products from a list of preset categories. Therefore, while donors estimate the size of their products, the actual product sizes are only revealed upon the arrival of the collection service. The majority of transported products are dry. Thus, the products may be considered homogeneous in terms of the vehicle capacity usage. Finally, such platforms often deploy collection services with volunteers (Curran and Williams 2010). Therefore, it is likely that not all products may be collected on a given day.

Another essential feature of the application under study is a certain repetition of the information process and problem parameters. Donors' requests are registered daily, from the same basin of donors, in a given time period called the *registration period*. At the end of this period, pickup operations are planned. Vehicle operations begin afterward. Thus, in essence, the DDCSs planning problem is rather similar from one day to another, except that the set of donors requesting service changes. On the other hand, statistical information on donors' locations and demands are generally available in the form of historical data. We refer to this feature by the term *variable customers*.

Our main objective is to develop a planning tool that can be adopted by DDCSs to program their collection activities. Given the nature of the application, this tool should capture the repetitive nature of the planning problem and should not require intensive daily computational effort. To achieve this, we first introduce a variant of the vehicle routing problem compatible with the previously described DDCS characteristics, which we call the Vehicle Routing Problem with a highly Variable Customer basis and Stochastic Demands (VRP-VCSD). We assume that the set of customers is variable and that customers may request service from anywhere within a given service area. We model the evolution of the information process as follows. First, since the service requests are received during the registration period, which precedes the planning and the dispatching period, we assume that customer locations and expected demands are known at the beginning of the planning phase. Second, the actual customer demand is observed upon visiting the customer. The VRP-VCSD then consists in dispatching a homogeneous fleet of vehicles initially located at the depot to serve the demands of the realized set of customers. Vehicles are allowed to perform so-called *preventive restocking* (see, for example [Louveaux and Salazar-González 2018](#)), thus enabling the possibility to return to the depot before the vehicle capacity is filled. Furthermore, similar to [Goodson, Ohlmann, and Thomas \(2013\)](#), [Goodson, Thomas, and Ohlmann \(2016\)](#), we assume that the fleet operates during a limited period of the day. Thus, a portion of demands may remain unserved, and the objective is then to maximize the total served demand. Such an objective is coherent with the DDCS nature.

Markov Decision Process (MDP) formulations provide a flexible and rich modeling framework for stochastic and dynamic decision problems. Given the complexity of the problem at hand and the variable customer feature, MDP formulations are particularly suited for the VRP-VCSD. Thus, we first propose an MDP model of the VRP-VCSD. This is a classical centralized model, where the decision-maker has full information on the vehicles' and clients' statuses and establishes the routes for all vehicles. The resulting model is, however, intractable even for small problem instances. The main challenge comes from the multi-vehicle nature of the VRP-VCSD and the consequent explosion in the dimension of the state and action spaces. Nonetheless, this model provides us with the ground to develop what we call a *partially decentralized* MPD formulation for the VRP-VCSD, which significantly reduces the dimension of the state and action spaces. The term decentralized is used in the literature to mean that the value function is computed for separated vehicle-specific action spaces ([OroojlooyJadid and Hajinezhad 2019](#)). Additionally, the partially decentralized formulation proposed in this paper has two main features. The first is based on the observation that two vehicles will choose the same action if they are in the same situation. As a result, instead of searching for one policy for each vehicle, we rather seek a unique policy that is applicable to all vehicles. As demonstrated in [Section 4](#), this is crucial for the success of the proposed algorithm. The second feature is that vehicles have access to the full state of the system, including the information about other vehicles (i.e., centralized). However, the global state is filtered via an *observation function*, which selects a subset of the information that is most relevant for a given vehicle, e.g., the set of closest customers. We note that although it is suggestive to think of the partially decentralized formulation in terms of self-deciding vehicles, the resulting policy may be operated in a central fashion. Indeed, in our approach, vehicles decide individually considering the status of all vehicles and customers, while maximizing the demand collected by all vehicles.

Among the available algorithms to solve routing problems expressed in terms of MDPs, we distinguish between two main families: *off-line* and *on-line* algorithms ([Ritzinger, Puchinger, and Hartl 2016](#)). In general, off-line methods invest most of the available computing time before operations start, and use the available information to provide an easy-to-use operational policy that can be repeatedly applied to many problem instances. On the contrary, on-line algorithms concentrate most of the computing efforts during operations taking advantage of the information revealed during operations. Given the repetitive nature of

our application, and the limited computational resources typical of DDCSs, we turn our attention to off-line methods. To find the resulting operational policy, we resort to Reinforcement Learning, and in particular, we implement a Q-learning algorithm (Watkins and Dayan 1992), which is an approximate and model-free form of the Value Iteration Algorithm for stochastic dynamic programming (Powell 2011) and it is an off-line algorithm. Q-learning enables estimating the value of each state-action pair via simulation. In its simplest form, states and actions are discrete, and state-action values are represented as a lookup table. However, this paper proposes a continuous state representation and incorporates a two-layer artificial neural network to approximate the Q values. The proposed algorithm, called DecQN, features two main key elements. First, the challenges of variable-sized customer sets are addressed by adopting a fixed-size vector based on a particular heatmap-style encoding technique. Second, given the proposed partially decentralized model and our choice to develop a single policy for all vehicles, our algorithm is only required to maintain a single set of Q values, which is iteratively updated according to the simulation data from all vehicles. Finally, we adopt several state-of-the-art techniques to improve the overall performance of our algorithm, including Replay Memory (Mnih et al. 2015) and Double Q Network (Van Hasselt, Guez, and Silver 2016).

We conduct a thorough computational analysis. First, given that no instance set is available for the VRP-VCSD in the literature, we construct a new instance set. We then implement three benchmark policies to compare with the DecQN. Results show that the DecQN considerably outperforms the considered benchmark policies. To provide a comparison with existing literature, we trained our DecQN on instances of the Vehicle Routing Problem with Stochastic Demand (VRPSD), which is a particular case of the VRP-VCSD where the customer set and expected demands are known in advance. Results show that even though our algorithm is not tailored to exploit the in-advance knowledge of customer locations, it is competitive with the current state-of-the-art algorithm of Goodson, Thomas, and Ohlmann (2016). Further computational analysis is then geared towards testing how the training phase of the DecQN can be guided towards generalization over different instances and problem dimensions, such as duration limits and stochastic variability. Finally, we show that the obtained policies can be easily employed in an *on-line* algorithm, thus further improving the performance of the DecQN.

To summarize, the contributions of the present work are as follows:

- We model the DDCSs by introducing the VRP-VCSD, which is a variant of the VRP with a variable customer basis and stochastic demand. For this new problem, we provide an MDP formulation based on the traditional centralized decision-making framework.
- We propose a partially decentralized MDP-based formulation of the VRP-VCSD, which entails searching for a single policy that is the same for all vehicles. This formulation enables us to develop computationally efficient state and action space aggregation strategies.
- We solve the VRP-VCSD via a state-of-the-art Q-learning algorithm, featuring recent accelerating strategies such as Replay Memory and Double Q Networks. This, in combination with the partially decentralized formulation, enables efficiently sharing simulated experiences among vehicles.
- We perform extensive computational experiments showing that the DecQN clearly outperforms three benchmarks for VRP-VCSD. Furthermore, when tested on instances of the VRPSD, DecQN is competitive with state-of-the-art methods specifically designed for that problem. Moreover, we show that the training phase of the DecQN can be generalized to tackle problem instances varying in terms of several dimensions, such as duration limits and stochastic variability. Finally, we show that the obtained off-line policies are suitable to be used as base policies in a Rollout Algorithm.

The paper is organized as follows. We provide a detailed literature review in Section 2. In Section 3, we describe the VRP-VCSD and provide the centralized MDP formulation. We then present the partially decentralized formulation in Section 4, describe the proposed algorithm in Section 5, and present our computational results in Section 6. Finally, we present our conclusions in Section 7.

2 Literature Review

We first review optimization problems related to the VRP-VCSD in Section 2.1. We then review MDP-based solution methods for stochastic routing problems in Section 2.2.

2.1 Related problems

The VRP-VCSD belongs to the family of Stochastic VRPs (SVRPs), which have been extensively studied in the literature (see [Oyola, Arntzen, and Woodruff \(2018, 2017\)](#) for a comprehensive review). The VRP-VCSD accounts for two sources of uncertainty; the first concerns the set of customers requesting the daily service, and the second concerns their demands. The literature addressing customer uncertainty can be classified in two main streams. In the first stream, a planner receives requests up until the beginning of the operations period, e.g., 8:00 AM. As the operations begin, no more requests are accepted, and the observed set of customers is served (e.g., [Bono et al. \(2020\)](#)). We refer to this form of uncertainty as *static* customers. In the second stream, a planner may continue receiving requests during the operations period and decides whether to accept or reject them (see, for example [Chen, Ulmer, and Thomas 2022](#), [Ulmer et al. 2017](#)). We refer to this form of uncertainty as *dynamic* customers.

Among SVRPs with static customers, we further distinguish between two categories, according to the assumptions made about the set of potential customers. The first category assumes that the set of potential customers is fixed and known in advance (e.g., [Gendreau, Laporte, and Séguin \(1995\)](#)). In this setting, only a subset of customers is “present” each day. Given that the customer set is known in advance and does not change from one day to another, we denote this as the *fixed* customer assumption. It is worth noting that several works on stochastic versions of the Traveling Salesman Problem share this modeling framework, such as [Voccia, Campbell, and Thomas \(2013\)](#). Conversely, the second category of works assumes that customers may request service from any location in a given service area (e.g., [Lin, Ghaddar, and Nathwani \(2021\)](#), [Bono et al. \(2020\)](#)). As previously mentioned, we refer to this feature as variable customers.

Works focusing on demand uncertainty generally assume that the set of customers requesting service is known in advance, i.e., fixed. Within this stream, we identify two main problem settings. In the first, vehicles must fully serve all customer demands. Due to the uncertainty of the latter, vehicles may have to return to the depot to reload and continue the service. In such cases, the objective is to minimize the expected total costs, which includes returns to the depot (e.g., [Louveaux and Salazar-González \(2018\)](#)). In the second stream, similarly to the VRP-VCSD, a deadline on the duration of the operations is considered. [Mendoza, Rousseau, and Villegas \(2016\)](#) assume a soft deadline and penalize late services. Other authors do not allow late services, and in particular in [Erera, Morales, and Savelsbergh \(2010\)](#), additional vehicles might be dispatched if needed, while in [Goodson, Ohlmann, and Thomas \(2013\)](#), [Goodson, Thomas, and Ohlmann \(2016\)](#) not all customers might be served, and the objective is to maximize the total demand served within the deadline.

The VRP-VCSD belongs to the category of SVRPs with static and variable customers, and additionally considers a second layer of uncertainty on customer demands. To the best of our knowledge, this problem setting has not been previously addressed in the literature.

2.2 Solution methods

MDP formulations are commonly used to model SVRPs. This section reviews solution methods for the SVRP with stochastic customers and/or demands. We label the corresponding literature as MDP-based solution methods. We focus on Approximate Dynamic Programming (ADP), Reinforcement Learning (RL), and Multi-agent Reinforcement Learning. For a more general discussion, the reader is referred to [Soeffker, Ulmer, and Mattfeld \(2022\)](#). Table 1 summarizes the literature that is most relevant to our work. The first part of Table 1 reports works with a single-vehicle, whereas the second part reports works with multi-vehicles. The multi-vehicle nature of the VRP-VCSD requires considerably more complex methods. Thus, our review focuses on how large action and state spaces are addressed in multi-vehicle problems.

We classify MDP-based methods according to the approach used in making routing decisions. The first approach determines, at each *decision epoch*, the next customer each vehicle should visit by optimizing an estimated value function (see, for example Maxwell et al. 2010, Oda and Joe-Wong 2018, Chen et al. 2019). Conversely, at each decision epoch, the second approach maintains a temporary route of which only the first customer is retained. These routes are dynamically updated at each decision epoch. The first approach provides a simple and effective way to tackle routing problems with variable customers, such as Oda and Joe-Wong (2018), Chen et al. (2019). Therefore, we adopt this approach in this paper. The second approach is more suited to situation where customer locations are known in advance, such as Goodson, Ohlmann, and Thomas (2013), Goodson, Thomas, and Ohlmann (2016), or in dynamic customer settings, (e.g., Ulmer (2020), Joe and Lau (2020)). We remark that solution methods may also combine these two strategies, as for example, Kullman et al. (2021) where a ride-hailing problem is addressed.

Reference	Problem	Obj. Func.	Uncert.		Fleet	TL	RD	Appr.	Coord.	Solution method (comp.)
			Cust.	Other						
Secomandi (2001)	SVRP	min TT	F	D	S	-	RB	-	-	RA (On.)
Novoa and Storer (2009)	SVRP	min TT	F	D	S	-	RB	-	-	RA (On.)
Peng, Wang et al. (2020)	SVRP	min C	V	-	S	-	N	-	-	PG + AM (Off.)
Brinkmann, Ulmer, and Mattfeld (2019a)	SIRP	min No. SF	F	D	S	-	N	-	-	H (On.)
Ulmer et al. (2017)	DVRP	max No. SR	D	-	S	L	RB	-	-	RA + VFA (On.-Off.)
Nazari et al. (2018)	DVRP	max SD	D	-	S	TW	N	-	-	PG + AM (Off.)
Fan, Wang, and Ning (2006)	SVRP	min TT	F	D	M	-	RB	DP	×	RA (On.)
Goodson, Ohlmann, and Thomas (2013)	SVRP	max SD	F	D	M	L	RB	DP	×	RA (On.)
Goodson, Thomas, and Ohlmann (2016)	SVRP	max SD	F	D	M	L	RB	DP	×	RA (On.)
Bono et al. (2020)	SVRP	min C	V	T	M	TW	N	DC	CR	PG + AM (Off.)
Lin, Ghaddar, and Nathwani (2021)	SVRP	min C	V	-	M	TW	N	-	-	PG (Off.)
Li et al. (2021a)	SVRP	min TT	V	-	M ¹	TW	N	-	-	PG + AM (Off.)
Brinkmann, Ulmer, and Mattfeld (2019b)	SIRP	min No. SF	F	D	M	-	N	DC	AP	H (On.)
Joe and Lau (2020)	DVRP	min C	D	-	M	TW	RB	DC	AP	SA + VFA (On.-Off.)
Chen, Ulmer, and Thomas (2022)	SDD	max No. SR	D	-	M ¹	-	RB ²	-	-	Q-learning + H (On.-Off.)
Ulmer (2020)	SDD	max R	D	-	M	L, TW	RB	DP	×	H + VFA (On.-Off.)
Li et al. (2021b)	PDVRP	min C	D	-	M	TW	RB	DP	AP	Q-learning (On.-Off.)
Kullman et al. (2021)	DARP	max P	D	-	M	L, TW	RB + N	DC	SR	Q-learning (Off.)
Maxwell et al. (2010)	DRP	min No. DS	D	-	M	TW	N	DC	CR	API (Off.)
Oda and Joe-Wong (2018)	DRP	min No. RR + IT	D	-	M	TW	N	DC	×	Q-learning (Off.)
Chen et al. (2019)	DRP	max R	D	-	M	TW	N	DC	SR	H + PG (On.-Off.)
Li et al. (2019)	DRP	max R	D	-	M	-	N	DC	SR	Q-learning (Off.)
Our research	SVRP	max SD	V	D	M	L	N	DC	CR	Q-learning (Off.)

Table 1: MDP-based solution methods proposed for routing problems

¹: Heterogeneous vehicles

- ²: The decision in the MDP formulation is to either reject or choose a vehicle/drone to assign that request. Then, a heuristic decides how to accommodate that request in the route.
- Problem: Stochastic VRP (SVRP), VRP with Dynamic Requests (DVRP), Dispatching and Re-positioning Problem (DRP), Dial-A-Ride Problem (DARP), Stochastic Inventory Routing Problem (SIRP), Same-Day Delivery (SDD), Pick-up and Delivery VRP (PDVRP)
 - Obj. Func.: The Objective Function can be min of Travel Time (min TT), Number of Delayed Services (min No. DS), Costs (min C), Number of Rejected Requests (min No. RR), Number of Service Failures (min No. SF), and Idle Time (min IT), or max of Served Demand (max SD), Profit (max P), Revenue (max R), and Number of Served Requests (max No. SR)
 - Uncert.:
 - Cust.: Customers can be Static and Fixed (F), Static and Variable (V), or Dynamic (D)
 - Other: Other sources of uncertainties can be Demand (D) or Travel Time (T)
 - Fleet: Single vehicle (S), Multiple vehicles (M), and Unlimited vehicles (U)
 - TL: Time limits including, a duration limit for the operation (L), or Time Windows for customers (TW)
 - RD: The routing decision is Where to go next (N) or Route-based (RB)
 - Appr.: The approach to cope with complexities of the MDP: Decompose the problem into multiple single-vehicle problem (DP), Decentralize the action space (DC)
 - Coord.: How decentralized vehicles are coordinated: with Collective Rewards (CR), Shaped Rewards (SR), Assignment Problem (AP), or No coordination (×)
 - Solution method (comp.): Rollout Algorithm (RA), Approximate Policy Iteration (API), Simulated Annealing (SA), Value Function Approximation (VFA), Heuristics (H), Policy Gradient (PG), Attention Mechanism (AM). comp.: indicates how/when the majority of computation is done, On-line (On) or Off-line (Off).

MDP formulations are generally solved by Dynamic Programming algorithms. These, however, suffer from the so-called curse of dimensionality. In multi-vehicle SVRPs, typically featuring very large combinatorial state and decision spaces, this curse is further aggravated. Several approaches have been proposed to cope with these difficulties. Fan, Wang, and Ning (2006) and Goodson, Ohlmann, and Thomas (2013) decompose the problem into multiple single-vehicle problems. Fan, Wang, and Ning (2006) use a myopic heuristic technique to partition customers into m subsets, one for each available vehicle. Once the subsets are established, they are kept fixed during the execution of the algorithm. Goodson, Ohlmann, and Thomas (2013) refine this technique by dynamically re-partitioning customers at each decision epoch. While both approaches drastically reduce the action and state spaces, collaboration opportunities among vehicles are not explicitly enforced.

As previously mentioned, an alternative approach to reduce the curse of dimensionality is to decentralize the decision space. We recall that the term decentralize entails that the value function is computed for separated vehicle-specific action spaces rather than for the joint action space (OroojlooyJadid and Hajinezhad 2019). This approach is based on two main hypotheses: 1) once a vehicle is assigned to a destination, it is never diverted to another destination, even if this is favorable in light of new information, and 2) at any decision epoch, it is unlikely that more than one vehicle needs to be assigned to a new destination. The simplest way to handle decentralization is to optimize the individual reward of each vehicle, regardless of the impact on the performance of other vehicles. However, this is equivalent to ignoring cooperation among vehicles, which may lead vehicles to compete for the reward. For example, Oda and Joe-Wong (2018) study a dynamic fleet management problem for taxi dispatching and re-positioning where assignments of taxis to customers are determined to maximize the number of requests a given taxi can individually serve.

The task of achieving some level of collaboration in a decentralized framework is very challenging and it has been extensively studied in the literature of multi-agent systems (OroojlooyJadid and Hajinezhad 2019). One possible strategy is to solve, at each decision epoch, an auxiliary master problem accessing information from the value functions of each individual vehicle. For example, in the context of a bike-sharing system, Brinkmann, Ulmer, and Mattfeld (2019b) first compute the number of expected unserved requests for each individual vehicle if assigned to each of the bike stations and then deploy a greedy algorithm to solve an assignment problem minimizing the total expected number of unserved requests. For a VRP with dynamic customers, where requests are dynamically assigned to vehicles, Joe and Lau (2020) develop an approximated value function to estimate the cost of each individual vehicle route and then adopt a Simulated Annealing algorithm to search for an assignment minimizing the expected total cost. An alternative strategy is to shape the individual rewards to account for the influence of the vehicle’s actions on the overall system performance (Li et al. 2019, Chen et al. 2019, Kullman et al. 2021). This strategy implicitly favors vehicle coordination. For example, in an order dispatching problem, Li et al. (2019) model the reward function as a weighted sum of the prize collected by the vehicle, while accounting for potential future rewards from other vehicles.

In our work we consider an alternative strategy. On the one hand, we enforce the sequentialization of the decision process, as in Maxwell et al. (2010), Bono et al. (2020), i.e., we determine the action for one vehicle at a time. Additionally, we impose that the single-vehicle policy must be the same for *all* vehicles. In this context, the value function represents the reward-to-go that vehicles may *collectively* earn.

Although decentralizing significantly reduces the action space, the state space remains challenging. Various techniques have been introduced to handle this issue. For example, Ulmer, Mattfeld, and Köster (2018), Joe and Lau (2020), Maxwell et al. (2010) replace the actual state with a set of basis functions. Alternatively, Kullman et al. (2021), Chen et al. (2019) aggregate customers’ information by a grid-like discretizing of the service region. Other works combine grid-like discretization with the assumption that vehicles cannot fully observe the current state. For example, in a ride-sharing application, Li et al. (2019) assume that vehicles can only access trip requests information located within a given range from their current position. The aggregation technique we propose in this paper is a combination of the previous ones. We aggregate customers’ information using a grid-like discretization, we represent a subset of customers by basis functions, and we use a vehicle-specific *observation* function to return a simplified representation of the state. Recently, new techniques involving the adoption of Deep Neural Networks have been proposed (see Bono et al. 2020, Li et al. 2021a, for example). Although these techniques seem promising, their implementation is computationally very expensive and usually requires complex tuning procedures.

Two main methodologies have been adopted to solve SVRPs expressed by MDP formulations. Approximate Policy Iteration (API) methods, such as Policy Gradient, aim at directly developing the desired policy by iteratively improving an initial policy (e.g., Bono et al. (2020)). We observe that the on-line Rollout Algorithm, such as the one developed in Goodson, Ohlmann, and Thomas (2013), can be viewed as a single iteration of the Policy Iteration algorithm (Bertsekas 2013). On the other hand, Approximate Value Iteration (AVI) methods, such as Q-learning, compute a value function, from which it is straightforward to derive the

corresponding policy (e.g., [Chen, Ulmer, and Thomas \(2022\)](#), [Li et al. \(2021b\)](#)). We choose to implement a Q-learning algorithm.

To conclude, MDP-based methods are promising for SVRPs. To the best of our knowledge, no existing MDP-based method in the literature can be trivially adapted to the VRP-VCSD. Our work fills this gap.

3 The centralized VRP-VCSD

In [Section 3.1](#), we formally define the VRP-VCSD. In [Section 3.2](#), we introduce the centralized MDP formulation of the VRP-VCSD.

3.1 Problem definition

We consider a service area, where customers are located along with a depot denoted by l_0 . A set $\mathcal{V} = \{1, \dots, m\}$ of m homogeneous vehicles with capacity Q is initially placed at the depot. Customers may request service from any point in the service area. The set of customers requesting service \mathcal{C}_0 is revealed at the beginning of the operations period (e.g., every morning), with $n = |\mathcal{C}_0|$. Each customer $c \in \mathcal{C}_0$ is characterized by a location l_c , and a probabilistic demand whose expected value \bar{d}_c is assumed to be known. Accordingly, each customer is defined by a tuple of (l_c, \bar{d}_c) . The customer’s actual demand \hat{d}_c is only realized upon the first visit. We assume that the customer’s demand is splittable in the sense that, if a vehicle is unable to fully serve a visited customer, it will serve the customer as much as possible. The rest of the demand may be later served by the same vehicle or another one. The time taken to travel between locations i and j is assumed to be deterministic and is denoted $\tau_{i,j}$, for $i, j \in \{l_c | c \in \mathcal{C}_0\} \cup l_0$. Vehicles begin their trips at the depot, serve a certain subset of customers, and end their routes at the depot. Furthermore, vehicles must complete their operations before a given duration limit L . Vehicles may return to the depot during their trip for restocking operations after leaving a customer and before visiting the next one, even if the vehicle capacity has not been filled yet. Although our problem is to pick up items, we use the term *restocking* to refer to such a policy as is typical in the literature ([Louveaux and Salazar-González 2018](#)). However, in our case, restocking entails emptying the vehicle capacity. The objective is to maximize the expected total amount of served demand.

3.2 The centralized formulation

We now provide a centralized MDP formulation of the VRP-VCSD. We use the term centralized to refer to the classical approach, where routes are built by one central decision-maker. An MDP formulation generally consists of a *state* which represents the current status of the system, a control *action*, and a function describing the transition of the system to a new state once an action is taken and exogenous information is revealed. In our centralized MDP formulation, the *decision epoch* is any point in time at which either a vehicle visits its destination, or when new information is revealed. This includes i) the beginning of the horizon, when the set of customers is revealed, and ii) during operations, when at least one vehicle arrives at a customer, or when a vehicle arrives at the depot. At each decision epoch k , the status of the system is represented by a state s_k as follows:

$$s_k = ([l_c, h_c, \bar{d}_c, \hat{d}_c]_{c \in \mathcal{C}_0}, [l_v, a_v, q_v]_{v \in \mathcal{V}}, t_k), \quad (1)$$

where the first two groups of components refer to the state of customers and vehicles, respectively, and the last component indicates the time. Note that although the customer and vehicle state components are naturally indexed by the decision epoch k , we have simplified the notation by omitting the index k . The state of each customer $c \in \mathcal{C}_0$ is represented by a tuple of $(l_c, h_c, \bar{d}_c, \hat{d}_c)$. The customer’s availability h_c takes value 1 if the customer is available to be served and 0 once it has been completely served. The customer’s availability h_c takes value 1 if the customer is available to be served and 0 once it is assigned to a vehicle or it has been completely served. For each vehicle $v \in \mathcal{V}$, the tuple of (l_v, a_v, q_v) forms its state, where l_v , a_v , and q_v are the destination (i.e., the location the vehicle is heading to), arrival time at destination, and the current available capacity, respectively. The time of the system at decision epoch k is denoted by t_k .

The action set is represented by an m -dimensional vector of $x_k = (x_k^1, \dots, x_k^m)$, where x_k^v indicates the next location vehicle v travels to at decision epoch k . Let $\bar{\mathcal{V}}_k = \{v \in \mathcal{V} | a_v = t_k\}$ be the set of active vehicles that arrive at their destinations and are available to take action at decision epoch k . At decision epoch k , the action x_k belongs to the action space $A(s_k)$ defined as:

$$A(s_k) = \{x_k \in \{\mathcal{C}_0 \cup \{l_0\}\}^m : \quad (2)$$

$$x_k^v = l_v, \quad \forall v \in \mathcal{V} \setminus \bar{\mathcal{V}}_k, \quad (3)$$

$$x_k^v = l_0, \quad \forall \{v \in \bar{\mathcal{V}}_k | q_v = 0\}, \quad (4)$$

$$x_k^v \neq x_k^{v'}, \quad \forall \{v, v' \in \mathcal{V} | v \neq v', x_k^{v'} \neq l_0\}, \quad (5)$$

$$x_k^v \in J(s_k, v) \cup \{l_0\}, \quad \forall v \in \bar{\mathcal{V}}_k, \quad (6)$$

$$x_k^v \neq l_0, \quad \forall \{v \in \bar{\mathcal{V}}_k | J(s_k, v) \setminus X_k^{-v} \neq \emptyset, l_v = l_0\}, \quad (7)$$

where $X_k^{-v} = \{x_k^1, \dots, x_k^{v-1}, x_k^{v+1}, \dots, x_k^m\}$ denotes the set of actions at time k for all vehicles except vehicle v , and $J(s_k, v)$ the set of reachable customers by vehicle v that have not been completely served. Thus,

$$J(s_k, v) = \{c \in \mathcal{C}_0 | h_c = 1, \tau_{l_v, l_c} + \tau_{l_c, l_0} \leq L - t_k\}. \quad (8)$$

In the defined action space $A(s_k)$, Condition (3) enforces the fact that vehicles cannot be relocated when assigned to a destination. Condition (4) implies that vehicles with no available capacity should return to the depot to replenish. Condition (5) ensures that no two vehicles can choose the same destination unless the destination is the depot, while Condition (6) ensures that vehicles travel to reachable customers in $J(s_k, v)$ or to the depot. Finally, Condition (7) entails that waiting in the depot is only allowed when there are no available customers to visit.

The information about customers' presence and demand volumes is revealed in two phases. At the first decision epoch ($k = 0$), no customer is realized yet. Thus, $s_0 = ([\cdot], [(l_0, 0, Q)]_{v \in \mathcal{V}}, t_0)$. At this point, a dummy action $x_0 = (l_0)_{v \in \mathcal{V}}$ transfers the system to the next decision epoch ($k = 1$) where the system time and the vehicle states remain the same; however, the set of realized customer locations and expected demands populates the set of customers \mathcal{C}_0 . Consequently, we have: $s_1 = ([l_c, 1, \bar{d}_c, -1]_{c \in \mathcal{C}_0}, [(l_0, 0, Q)]_{v \in \mathcal{V}}, t_1)$. For each realized customer $c \in \mathcal{C}_0$, we set \hat{d}_c to -1 at the beginning and will update it upon its first visit. Also, h_c is initially set to one for all customers.

It is worth noting that the way the state s_0 is initialized highlights one of the main features of the VRP-VCS D. In this MDP formulation, we develop a policy accounting for all possible customer realizations, which can tackle realizations that have never been seen before. Accordingly, the system starts with no customers, and a random set of customers will be revealed in decision epoch 1. For $k \geq 1$, \mathcal{C}_0 is assumed to be fixed. Let w be a sample scenario of customer demands and $w_k \subset w$ be the set of realized demand volumes of those customers whose actual demands are observed at decision epoch k . By taking the action x_k from the set $A(s_k)$ of possible actions in the state s_k , the system transits to the next state $s_{k+1} = S^M(s_k, x_k, w_{k+1})$, where $S^M(\cdot)$ is a two-step transition function. In the first step, the post-decision state s_k^x is the state immediately after taking action x_k , but before revealing the exogenous information w_{k+1} :

$$h_{x_k^v} = 0, \quad \forall \{v \in \bar{\mathcal{V}}_k | x_k^v \neq l_0\}. \quad (9)$$

$$a_v = t_k + \tau_{l_v, l_{x_k^v}}, \quad \forall v \in \bar{\mathcal{V}}_k. \quad (10)$$

$$l_v = l_{x_k^v}, \quad \forall v \in \bar{\mathcal{V}}_k. \quad (11)$$

$$t_{k+1} = \min_{v \in \mathcal{V}} a_v. \quad (12)$$

Equation (9) flags the chosen customers as unavailable. The arrival time as well as the location of active vehicles are updated using Equations (10) and (11). Finally, Equation (12) establishes the time of the next decision epoch, where the exogenous information w_{k+1} will be revealed. All the other components are left unmodified. The second step of the transition function happens at the beginning of a new decision epoch

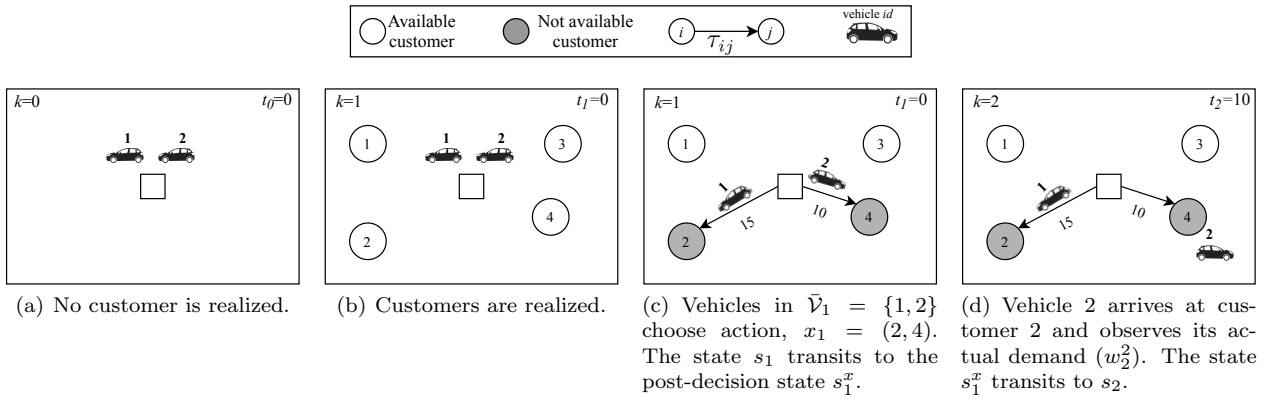


Figure 1: The transition function in a centralized MDP formulation

$(k + 1)$ by transiting from the post-decision state s_k^x to the next state s_{k+1} . Let $\tilde{\mathcal{C}}_{k+1} = \{c \in \mathcal{C}_0 \mid \exists v \in \bar{\mathcal{V}}_{k+1} \wedge l_c = l_v\}$ be the set of customers that are served at decision epoch $k + 1$. If the actual demand of a customer in $\tilde{\mathcal{C}}_{k+1}$ is not yet realized ($\hat{d}_c = -1$), its value will be set to the observed demand w_{k+1}^c .

$$\hat{d}_c = w_{k+1}^c, \quad \forall \{c \in \tilde{\mathcal{C}}_{k+1} \mid \hat{d}_c = -1\}. \quad (13)$$

Let η_v^{k+1} be the demand volume that vehicle $v \in \bar{\mathcal{V}}_{k+1}$ serves at decision epoch $k + 1$, defined as:

$$\eta_v^{k+1} = \min\{\hat{d}_{c_v}, q_v\}, \quad \forall \{v \in \bar{\mathcal{V}}_{k+1} \mid l_v \neq l_0\}, \quad (14)$$

where c_v refers to a customer $c \in \tilde{\mathcal{C}}_{k+1}$ that is served by vehicle v (i.e., $l_c = l_v$). The unserved demands of customers in $\tilde{\mathcal{C}}_{k+1}$ and the available capacity of vehicles in $\bar{\mathcal{V}}_{k+1}$ are then updated as follows:

$$\hat{d}_{c_v} = \hat{d}_{c_v} - \eta_v^{k+1}, \quad \forall \{v \in \bar{\mathcal{V}}_{k+1} \mid l_v \neq l_0\}. \quad (15)$$

$$q_v = \begin{cases} q_v - \eta_v^{k+1} & \text{if } l_v \neq l_0, \\ Q & \text{otherwise.} \end{cases} \quad \forall v \in \bar{\mathcal{V}}_{k+1}. \quad (16)$$

Customers in $\tilde{\mathcal{C}}_{k+1}$ whose demands are not fully served will continue being available for service. Thus,

$$h_c = 1, \quad \forall \{c \in \tilde{\mathcal{C}}_{k+1} \mid \hat{d}_c > 0\}. \quad (17)$$

These two steps are illustrated in Figure 1, which displays an example with four customers and two vehicles.

We define the terminal decision epoch K as the point in time at which all vehicles are located at the depot, and vehicles have no other choice than to stay at the depot due to the duration limit L ($A(s_K) = \{(l_0)_{v \in \mathcal{V}}\}$). The reward function $R(s_k, x_k, w)$ is defined as the demands served by taking action x_k in state s_k , and the exogenous information w is observed:

$$R(s_k, x_k, w) = \sum_{\{v \in \bar{\mathcal{V}} \mid x_k^v \neq l_0\}} \min\{q_v, d_{x_k^v}^w\} \quad (18)$$

$$d_c^w = \begin{cases} w_k^c & \text{if } \hat{d}_c = -1, \\ \hat{d}_c & \text{otherwise.} \end{cases} \quad \forall c \in \mathcal{C}_0, \quad (19)$$

where w_k^c is the demand of customer c observed when the vehicle v visits the customer c at decision epoch \bar{k} . The decision epoch \bar{k} corresponds to the point in time when the vehicle $v \in \bar{\mathcal{V}}$, which has selected customer x_k^v at the decision epoch k , arrives at its destination: $\bar{k} = \{k' \in [0, \dots, K] \mid t_{k'} = t_k + \tau_{l_v, l_{x_k^v}}\}$. Thus, the collection of the reward is generally delayed.

The value of being in state s_k is defined as $V(s_k)$. This function indicates the expected cumulative reward the system can collect from state s_k onward:

$$V(s_k) = \max_{x_k \in A(s_k)} \mathbb{E}_w [R(s_k, x_k, w) + \gamma V(s_{k+1})]. \quad (20)$$

In Equation (20), similar to Kullman et al. (2021), we consider the discount factor γ attributing greater importance to immediate rewards.

There are some challenges making this formulation intractable for the VRP-VCSD. First, the dimension of the state representation is dependent on the cardinality of customers, which is stochastic. Consequently, the size of the vector s_k would be variable and dependent on the number of realized customers, preventing the use of many solution methods that assume a fixed-size state. For example, no linear regression method can be implemented to approximate the value function in Equation (20), when the size of the input (state vector) is variable. Furthermore, given the potentially large number of customers and the fact that the state of customers is represented by continuous variables, the state space is tremendously large. On the other hand, managing multiple vehicles makes the size of the action space, defined in Equations (2)–(7), excessively large. If we consider \underline{n} customers available to be served at decision epoch k , the size of the action space is $\frac{\underline{n}!}{(\underline{n}-m)!}$. Handling such a large action set is computationally prohibitive. The following section explains how the partially decentralized formulation allows us to cope with these challenges.

4 The partially decentralized VRP-VCSD

The MDP formulation proposed in this section is decentralized as the action-space is decomposed by vehicle. However, the decentralization is not complete because 1) we enforce that all vehicle-specific policies are the same, 2) even though filtered by an observation function (see details in Section 4.2), we assume that vehicles access information on the global state of the system, and 3) the optimization is done over the joint policy that is obtained as the union of the vehicle-specific policies, thus the resulting value function represents the collective reward. To facilitate the decomposition of the action-space, we enforce that only one vehicle, called the *active vehicle*, is allowed to make a decision at a given decision epoch.

The resulting formulation has three main advantages. First, since the decision is restricted to one vehicle only, the size of the action space is drastically reduced to \underline{n} (from potentially up to $\frac{\underline{n}}{(\underline{n}-m)!}$), where \underline{n} is the number of available customers in the current decision epoch. Second, while preserving the global state of the system, the formulation allows us to filter the information that is more relevant for the active vehicle (via the observation function). This substantially reduces the size of the state space, when compared to the centralized case. Third, the global policy is comprised of the union of vehicle-specific policies, which are forced to be identical. Thus, the approach has only to optimize a single policy (which is shared by all vehicles), instead of m policies.

We derive the partially decentralized formulation in Section 4.1. In Section 4.2, we provide a detailed description of the vehicle observation function and its encoding.

4.1 The partially decentralized formulation

We define two levels of state representation. The first is the *global state* s_k , which we presented in the centralized MDP formulation. This keeps track of the evolution of the entire system. In the second level, we introduce the observation function $O(s_k, \bar{v})$, which takes as input the global state s_k and the current active vehicle \bar{v} , and returns $o_{k,\bar{v}}$, which is the state as observed by vehicle \bar{v} . The observation $o_{k,\bar{v}}$ is comprised of four parts:

$$o_{k,\bar{v}} = [F_k | H_k | G_k | t_k], \quad (21)$$

where F_k is the state of a subset of customers that are promising for \bar{v} , H_k is an aggregated overview of all customers in the service area, $G_k = [(l_v, a_v, q_v)]_{v \in \mathcal{V}}$ is the state of all vehicles, and t_k is the time at decision epoch k . We detail the components of the observation function in Section 4.2.

Only one vehicle at a time is allowed to make a decision. If multiple vehicles are active at decision epoch k , one is randomly chosen as \bar{v} . We redefine the action and the action space for \bar{v} as $x_k = (x_k^{\bar{v}})$ and $A(s_k, \bar{v})$. Namely,

$$A(s_k, \bar{v}) = \{x_k \in \{J(s_k, \bar{v}) \cup \{l_0\}\} : \quad (22)$$

$$x_k = l_0 \quad \text{if } q_{\bar{v}} = 0, \quad (23)$$

$$x_k \neq l_0 \quad \text{if } J(s_k, \bar{v}) \neq \emptyset, l_{\bar{v}} = l_0\}, \quad (24)$$

where Condition (22) obliges x_k to be a customer from the set of feasible customers $J(s_k, \bar{v})$ or the depot, Condition (23) forces the active vehicle to travel to the depot when it has no remaining capacity, and Condition (24) does not allow the vehicle to stay at the depot if there are reachable customers to be served. Furthermore, the reward of taking action x_k when the active vehicle \bar{v} observes $o_{k,\bar{v}}$ is denoted by $R(o_{k,\bar{v}}, x_k, w)$ and remains equal to the reward function in the centralized formulation $R(s_k, x_k, w)$, if $\bar{\mathcal{V}}_k = \{\bar{v}\}$.

As previously mentioned, we use the global state s_k to keep track of the system dynamic. Therefore, the state transition function $S^M(\cdot)$ and its associated equations (Equations (9)–(17)) are still applicable here, given that $\bar{\mathcal{V}}_k = \{\bar{v}\}$. Given the observation of the global state is $o_{k,\bar{v}}$, we aim at finding a policy π that indicates the best location to travel to for the active vehicle \bar{v} in the feasible action space $A(s_k, \bar{v})$. The resulting policy selects actions such that the total served demand by all vehicles is maximized. The optimal policy π^* is obtained by solving the following equations:

$$V^\pi(o_{k,\bar{v}}) = \max_{x_k \in A(s_k, \bar{v})} \mathbb{E}_w[R(o_{k,\bar{v}}, x_k, w) + \gamma V(o_{k+1, \bar{v}'})], \quad (25)$$

$$\pi^*(o_{k,\bar{v}}) = \arg \max_{x_k \in A(s_k, \bar{v})} \mathbb{E}_w[R(o_{k,\bar{v}}, x_k, w) + \gamma V(o_{k+1, \bar{v}'})], \quad (26)$$

where \bar{v}' is the active vehicle in decision epoch $k+1$ and $V(o_{k,\bar{v}})$ is the expected reward-to-go starting from observation $o_{k,\bar{v}}$ onward. In the terminal global state s_K , there is no customer available to be served. Hence, $V^\pi(o_{K,v}) = 0, \forall v \in \mathcal{V}$.

4.2 The observation function and its representation

The primary purpose of the observation function is to suitably select the most relevant information for the active vehicle and aggregate the remaining information. To this purpose, we identify a subset of *target customers* $\mathcal{C}_{\bar{v}} \subset \mathcal{C}_0$ which we deem as more promising for the active vehicle. Therefore, instead of keeping detailed information for all customers, the observation function only maintains the comprehensive information of target customers and aggregates the rest.

Considering our problem setting, we identify two desired characteristics for the target customers $c \in \mathcal{C}_{\bar{v}}$: requesting large demand volumes (d_c), and being close to the active vehicle ($\tau_{l_c, l_{\bar{v}}}$). Therefore, we define a new measure to identify \tilde{n} target customers, where \tilde{n} is an input. We choose \tilde{n} customers with higher $\rho_{c,\bar{v}} = \frac{\min(\tilde{d}_c, q_{\bar{v}})}{\tau_{l_c, l_{\bar{v}}}}$, with $\tilde{d}_c = \bar{d}_c$ for $\hat{d} = -1$, and $\tilde{d}_c = \hat{d}_c$ otherwise. This measure normalizes the customers' demands by their distance to the active vehicle, and also accounts for the available capacity. The effectiveness of selecting target customers according to their score $\rho_{c,\bar{v}}$ was validated through preliminary computational tests.

In order to maintain information related to target customers, we represent each customer using a set of features as $(l_c, \tau_{l_c, l_{\bar{v}}}, \tau_{l_c, l_0}, \tilde{d}_c, \min(\tilde{d}_c, q_{\bar{v}}), \mu_c)$. In this feature set, l_c refers to the customer's location, $\tau_{l_c, l_{\bar{v}}}$ is the travel time between the customer and the active vehicle, τ_{l_c, l_0} is the travel time between the customer and the depot, \tilde{d}_c is the customer's unserved demand (or expected demand, if not realized yet), $\min(\tilde{d}_c, q_{\bar{v}})$ shows the portion of customer's demand that can be served by the active vehicle, and μ_c indicates whether the actual demand is realized or not. The vector of target customers is denoted as $F_k = [(l_c, \tau_{l_c, l_{\bar{v}}}, \tau_{l_c, l_0}, \tilde{d}_c, \min(\tilde{d}_c, q_{\bar{v}}), \mu_c)]_{c \in \mathcal{C}_{\bar{v}}}$.

We propose an aggregated representation of the remaining customers to provide the active vehicle with an overview of environment. The challenge here is that the stochastic customer set necessitates an aggregating technique that handles a variable number of inputs while delivering a fixed-size output. To this purpose, we propose a heatmap-style approach to encode all customers in the service area as a fixed-size vector H_k . In particular, we divide the service area into a set of square-shaped *partitions* P . Let $\mathcal{C}_p \subset \mathcal{C}_0$ be the subset of customers that are located in $p \in P$. We characterize each p by (ξ_p^c, ξ_p^d) representing the number of customers and the total expected demand in that partition, respectively. Thus, $\xi_p^c = |\mathcal{C}_p|$, $\xi_p^d = \sum_{c \in \mathcal{C}_p} \tilde{d}_c$, and

$$H_k = [(\xi_p^c, \xi_p^d)]_{p \in P}.$$

In addition to H_k and F_k , the state of the vehicles G_k forms the third segment of the observation representation (Equation (21)). We define $G_k = [(l_v, a_v, q_v)]_{v \in \mathcal{V}}$, which has the same representation used in the centralized state. Therefore, the main difference between s_k and $o_{k, \bar{v}}$ is the customers' state, with a variable size, replaced by a fixed-size vector $[F_k, H_k]$. Compared to the state representation s_k , the observation representation $o_{k, \bar{v}}$ has two advantages: it overcomes the problem of the variable-sized state and reduces the dimension of the observation. In particular, the customers' state in s_k is of dimension $4 * |\mathcal{C}_0|$, while $[F_k, H_k]$ is of dimension $(6 * \tilde{n} + 2 * |P|)$. For example, assuming an average number of customers of 50, the dimension of s_k is 200 on average. However, assuming $\tilde{n} = 10$ and $|P| = 25$, the dimension of $o_{k, \bar{v}}$ will be fixed at 110.

In addition to reducing and fixing the dimension of $o_{k, \bar{v}}$, using target customers reduces the dimension of the active vehicle's action space by limiting its actions to target customers. Therefore, in the definition of $J(s_k, \bar{v})$, which is used to construct the action space of the active vehicle, we substitute \mathcal{C}_0 with $\mathcal{C}_{\bar{v}}$. As a result, the size of the action space is reduced to $|\mathcal{C}_{\bar{v}}| + 1$, where $|\mathcal{C}_{\bar{v}}| \leq \tilde{n}$.

5 Solution method

Both the centralized and the partially decentralized formulations suffer from the so-called curse of dimensionality, which makes them difficult to be solved by conventional stochastic dynamic programming. Approximate methods have been proposed in the literature to overcome such challenges (Powell 2011). In this paper, we consider the Q-learning algorithm. Our preliminary experiments suggest that Q-learning is not able to solve the centralized formulation of the VRP-VCS. This can be explained by the large number of state-action pairs entailed by this formulation. Conversely, the partially decentralized formulation, having a considerably smaller state-action space, was more suitable to be addressed by Q-learning. We now detail the proposed algorithm for the partially decentralized formulation.

Q-learning enables learning the so-called Q factors of each state-action pair, through simulation. We provide a general overview of the Q-learning algorithm in Appendix A.1. The Q factor of a given state-action pair is defined as follows:

$$Q(s_k, x_k) = R(s_k, x_k, w) + \gamma \max_{x_{k+1} \in A(s_{k+1})} Q(s_{k+1}, x_{k+1}). \quad (27)$$

By adopting the partially decentralized formulation, we replace the state s_k by the observation $o_{k, \bar{v}}$, and rewrite the Equation (27) as follows:

$$Q(o_{k, \bar{v}}, x_k) = R(o_{k, \bar{v}}, x_k, w) + \gamma \max_{x_{k+1} \in A(s_{k+1}, \bar{v}')} Q(o_{k+1, \bar{v}'}, x_{k+1}). \quad (28)$$

We denote $\hat{Q}(o_{k, \bar{v}}, x_k)$ as the estimation of $Q(o_{k, \bar{v}}, x_k)$, and use it to update the Q factor of a given state-action pair by using the following equation:

$$Q(o_{k, \bar{v}}, x_k) \leftarrow Q(o_{k, \bar{v}}, x_k) + \alpha * [\hat{Q}(o_{k, \bar{v}}, x_k) - Q(o_{k, \bar{v}}, x_k)], \quad (29)$$

where \bar{v}' is the active vehicle at decision epoch $k + 1$.

We implement the Q values in the form of an artificial neural network instead of traditional look-up tables. This method is called Q-network in the literature, and returns the approximate Q value for a given

observation-action pair $(o_{k,\bar{v}}, x_k)$. For computational efficiency, it is desirable to design the Q-network in such a way that only one forward call is sufficient to return the Q values for all $(|\mathcal{C}_{\bar{v}}| + 1)$ actions in $A(s_k, \bar{v})$. To this purpose, we consider a neural network that returns $\tilde{n} + 1$ Q values in every call. Notice that, under some circumstances, the number of target customers can be less than \tilde{n} , making the cardinality of $A(s_k, \bar{v})$ variable, but restricted to $\tilde{n} + 1$. Therefore, in the vector of $\tilde{n} + 1$ Q values approximated by the Q-network, we associate the first $|\mathcal{C}_{\bar{v}}|$ values to the Q value of target customers $\mathcal{C}_{\bar{v}}$ and assign the last one to the depot. Q values not associated with target customers nor the depot will be set to 0.

We develop a neural network with two hidden layers. This network gets the observation representation $(o_{k,\bar{v}})$ as the input layer and returns approximate Q values in the output layer. We denote the size of the input and output layers by h^{in} and h^{out} , where $h^{in} = 6\tilde{n} + 2|P| + 3m + 1$ and $h^{out} = \tilde{n} + 1$. The hidden layers are assumed to be fully connected dense layers linked by an activation function (a rectified linear unit (ReLU)). The size of the hidden layers is chosen based on empirical tests. In particular, we set their sizes to $\lfloor \frac{2}{3}(h^{in} - h^{out}) \rfloor + h^{out}$ and $\lfloor \frac{1}{3}(h^{in} - h^{out}) \rfloor + h^{out}$, respectively. Figure 3 in Appendix A.2 illustrates the architecture of the proposed artificial neural network. Denoting by θ the trainable weights of the proposed neural network, the Q value of an observation-action pair is represented as $Q(o_{k,\bar{v}}, x_k, \theta)$. It is worth noting that any equation involving $Q(o_{k,\bar{v}}, x_k)$ will also apply to $Q(o_{k,\bar{v}}, x_k, \theta)$.

To train our network, we minimize the so-called loss function. We define this function based on the difference between the new estimation of the values $\hat{Q}(o_{k,\bar{v}}, x_k, \theta)$ and the current estimation $Q(o_{k,\bar{v}}, x_k, \theta)$, denoted as Δ (i.e., $\Delta = \hat{Q}(o_{k,\bar{v}}, x_k, \theta) - Q(o_{k,\bar{v}}, x_k, \theta)$). Among several loss functions used in the literature, we found that the Huber loss function performs better than the commonly used functions such as Mean Squared Error (MSE) and Mean Absolute Error (MAE). The Huber loss acts as an MSE for small Δ and as an MAE for larger Δ . The Huber loss is defined as:

$$Huber(\Delta) = \begin{cases} \frac{1}{2}\Delta^2 & \text{for } |\Delta| \leq \delta \\ \delta(|\Delta| - \frac{1}{2}\delta) & \text{otherwise,} \end{cases} \quad (30)$$

where δ is a control parameter. We obtained the best results by setting $\delta = 5$ and used the Adam optimizer (Kingma and Ba 2014) to update the network in order to minimize the loss function.

Algorithm 2 (in Appendix A.2) summarizes our DecQN algorithm. Similar to what was suggested by Mnih et al. (2015), our preliminary results showed that using the target network (Van Hasselt, Guez, and Silver 2016) and the replay memory accelerates convergence. By adopting the target network (parameterized by $\bar{\theta}$ in Algorithm 2), the model learns from a stable target. The target network $\bar{\theta}$ is periodically copied from the primary network θ every β_d trials. In the replay memory, experiences are stored in a First-In-First-Out list, denoted as B , with a fixed size. At every decision epoch, with a probability of β_t , a random batch of experiences (\tilde{B}) is sampled from this list to update the weights (θ) in the neural network. Several advantages have been mentioned for using the replay memory (Mnih et al. 2015) such as breaking the correlation between consecutive experiences and giving more chances to those experiences that happen more. The exploration rate (ϵ) and the learning rate (α) are linearly decayed during the training phase. The decaying rate is decided based on the length of the training process.

As previously mentioned, one of the main features of the proposed approach is that we only develop a single set of Q values, resulting in a policy shared among all vehicles. This has several advantages: On the one hand, the information learned by one vehicle via its interaction with the environment is shared with all other vehicles, thus accelerating the convergence of the algorithm. On the other hand, the resulting method is more sample efficient. Finally, maintaining and storing one policy is more manageable than maintaining m policies.

6 Experimental results

In this section, we present our computational experiments. Since no instance set is available in the literature, we construct a new set of instances for the VRP-VCSD. We design three main experiments. The first one,

presented in Section 6.1, is aimed at evaluating the overall performance of the DecQN algorithm. To this purpose, we implement three benchmarks, which we call Deterministic A Priori Policy (DAPP), Random Policy (RP), and Greedy Policy (GP). Given that DAPP requires solving a very complex deterministic optimization problem, we only test it on relatively small instances, and perform experiments on larger instances for the two other benchmarks. The purpose of the second experiment, presented in Section 6.2, is to compare the DecQN with the existing literature. The challenge is that no direct comparison is possible. The closest problem in the literature we are aware of, is the VRPSD for which Goodson, Thomas, and Ohlmann (2016) developed the current state-of-the-art method. As mentioned earlier, the VRPSD can be seen as a particular case of the VRP-VCSD where both customer locations and expected demands are known in advance. Even though our algorithm does not take advantage of the specific characteristics of the problem, it turns out that our algorithm is competitive and sometimes outperforms the results in Goodson, Thomas, and Ohlmann (2016). The third experiment, in Section 6.3, can be seen as an extension of the second one, where we investigate the possibility of modifying the training phase of the DecQN to develop a policy able to address a larger range of VRPSD instances aggregated over specific parameters, such as the duration limit and stochastic variability. Finally, an additional experiment providing a simple demonstration of the fact that the policies provided by our algorithm can be easily embedded as base policies in rollout algorithms, is presented in Appendix D. We note that depending on the size of the problem, training a policy according to Algorithm 2 takes 24 to 36 hours. Problems with fewer vehicles and customers or shorter duration limits, for example, demand less training time. The values of the hyper-parameters in Algorithm 2 and the computational environment are described in Appendix B.2.

6.1 Performance of DecQN in VRP-VCSD

We describe the main features of the instance set in Section 6.1.1, while Appendix B.1.1 provides the details of the instance generation method. The benchmarks policies DAPP, RP and GP are described in Section 6.1.2. We report the computational results in Section 6.1.3.

6.1.1 VRP-VCSD Instances

As custom when building computational experiments in learning-based methods, we need to provide two types of input data, one to be used in the training phase of the algorithm, the other in the testing phase. Elements of these two sets are samples of the problem at hand. Although training and testing sets are distinct, they are typically generated by sampling from the same distributions.

We define an instance i as the tuple $i = (\mathcal{A}, \Psi_{n_z}, \Psi_l, \Psi_{\bar{d}}, \Psi_{\hat{d}}, m, Q, L)$, where \mathcal{A} denotes the service area partitioned into a set of zones Z , while $\Psi_{n_z}, \Psi_l, \Psi_{\bar{d}}, \Psi_{\hat{d}}$ denote the probability distribution functions of the number of customers n_z per zone $z \in Z$ (customer density), customer locations, expected demands, and actual demands, respectively. Furthermore, m, Q, L indicate the number of vehicles, their capacity, and the duration limit, respectively. We detail the instance generation procedure in Appendix B.1.1. In particular, we consider five different distributions for the customer density Ψ_{n_z} (Very Low, Low, Moderate, High, and Very High), and three different values of the vehicle capacity Q (25, 50, and 75), resulting in a set I of 15 instances. Furthermore, the distribution Ψ_{n_z} determines the values of m and L (Appendix B.1.1). The resulting values of the tuple $(\Psi_{n_z}, \bar{n}, m, L)$ are (Very Low, 10, 2, 143.71), (Low, 15, 2, 201.38), (Moderate, 23, 3, 221.47), (High, 53, 7, 195.54), and (Very High, 83, 11, 187.29). Given an instance i , a realization \hat{i} (also referred to as a sample, or a scenario) is obtained by sampling from distributions $\Psi_{n_z}, \Psi_l, \Psi_{\bar{d}}, \Psi_{\hat{d}}$. The set of all realizations \hat{i} of i is denoted $\hat{I}(i)$.

6.1.2 Benchmarks

We now describe the benchmark policies. The DAPP assumes the knowledge of the customer locations and expected demands. It then constructs a set of routes, which are evaluated in the VRP-VCSD setting. To construct such routes, we formulate the deterministic counterpart of the VRP-VCSD (i.e., with realized customers and demands) by the MILP described in Appendix B.3. We find an initial set of routes by solving

this formulation for a given set of customers with demands corresponding to their expected values. We then evaluate the performance of these routes by simulating the classical recourse policy (i.e., once the vehicle capacity is exceeded a return trip to the depot is performed and the capacity of the vehicle is restored) for 100 demand realizations. The MILP was solved by CPLEX 20.1 with a time limit of two hours. Unlike the DecQN, which can be instantaneously executed for any set of customers (generated from a given distribution function), this benchmark requires a significant amount of time to find the fixed routes for each customer realization.

In the RP, an action is randomly picked from the action set. We compare with this policy since it is the policy that DecQN starts with when the exploration rate in the ϵ -greedy method is set to one. Therefore, the improvement of our model over RP demonstrates the effect of learning.

The GP chooses the customer $c \in A(s_k, \bar{v})$ with the highest \tilde{d}_c at each decision epoch. We recall that \tilde{d}_c provides the expected or the remaining demand of customer c . If several customers have the same \tilde{d}_c , the closer one is selected. As GP selects customers according to the potential reward in terms of served demands, it is thus aligned with the VRP-VCSO objective.

RP and GP are more comparable with our DecQN. However, they cannot handle preemptive restocking. Therefore, the action set is redefined as:

$$A(s_k, \bar{v}) = \begin{cases} \{l_0\} & q_{\bar{v}} = 0 \parallel J(s_k, \bar{v}) = \emptyset \\ J(s_k, \bar{v}) & \text{otherwise.} \end{cases} \quad (31)$$

6.1.3 Results and Discussion

As previously mentioned, the benchmark DAPP requires to solve a complex deterministic MILP for each customer realization. Given the two hours time limit we impose, the DAPP was only able to address instances with Very Low and Low densities. Therefore, we organize our discussion into two parts. In the first, we present instances with Very Low and Low densities, and compare DecQN with all three benchmarks. In this case, we also restrict the vehicle capacity to 25 and 50, given that for $Q = 75$ almost all demands could be served. In the second part, we compare the performance of DecQN with GP and the RP on instances with Moderate, High, and Very High densities.

The method to obtain the training and test sets is the same for each instance $i \in I$. In particular, the training set is obtained by sampling 5 million realizations \hat{i} from $\hat{I}(i)$. We then trained the DecQN on these realizations. The exploration rate decayed linearly from 1.0 to 0.1 in the first one million trials. The learning rate also decreased linearly from 10^{-3} to 10^{-4} in the first two million trials. As detailed below, due to computational limitations, the cardinality of the test for the first part is smaller than the test set of the second part. Note that although the training and the test sets are sampled from the same distributions, they are disjoint.

For each instance with Very Low and Low densities, the test set is obtained by generating ten customer realizations. For each customer realization, we then generate 100 demand realizations, resulting in 1000 scenarios. Table 2 shows the comparison based on average performance of DecQN, DAPP, RP, and GP. Extended results are presented in Table 11 in Appendix C. The first two columns in Table 2 indicate the characteristics of the instance, while columns n and $\mathbb{E} \sum d_c$ show the average number of customers and the average total expected demand. Column Opt. reports the number of customer realizations solved to optimality by the DAPP for each instance. The average total served demand by our proposed policy is reported in column DecQN. Column $\% \mathbb{E} \sum d_c$ shows the portion of all demands served by DecQN. Finally, the performance gap between DecQN and the three benchmarks is reported in columns %DAPP, %RP, and %GP, where measure %X, is computed as: $\%X = \frac{\text{DecQN} - X}{X} \times 100$.

The DAPP obtains optimal solutions in 17 out of 20 customer realizations on instances with Very Low density. This number decreases to 4 out of 20 for instances with Low density. Therefore, the values in Table

2 refer to realizations for which DAPP obtained optimal routes. DecQN outperforms DAPP by an average of 3.0%. This suggests that, when considering the Very Low and Low densities, even by giving the DAPP sufficient time to solve the resulting deterministic problem, our method is still a better choice. Furthermore, DecQN outperforms RP and GP by, an average, 41.5% and 19.9%. We note that such improvements increase for %RP and decrease for %GP with the density. This can be explained by the fact that, as the number of customers increases, the probability that RP deviates from the optimal solution increases. A denser instance, in contrast, is more favorable for GP. Intuitively, as instances become denser, the knapsack component of the problem becomes dominant, and greedy policies are known to behave well on these kind of problems.

According to Table 2, as the vehicle capacity becomes larger (from 25 to 50 in the Very Low density), the improvement over DAPP decreases (from 2.6% to 1.2%). To explain this finding, we remark that the vehicle capacity directly impacts the probability of route failure. When the capacity is larger, the routes are less vulnerable to failure caused by stochastic demands. Therefore, we argue that the advantage of our method over DAPP is more pronounced on instances with smaller capacity because our method can better handle route failures. Validating this finding for instances with Low customer density is not easy because only a few could be solved optimally.

Ψ_{n_z}	Q	n	Opt.	$\mathbb{E} \sum d_c$	DecQN	% $\mathbb{E} \sum d_c$	%DAPP	%RP	%GP
Very Low	25	10.4	17/20	105.0	68.9	66.3%	2.6%	34.8%	25.7%
	50				87.3	83.5%	1.2%	44.3%	15.7%
Avg							1.8%	40.0%	19.9%
Low	25	15.0	4/20	147.5	99.6	69.1%	2.3%	58.9%	14.3%
	50				122.0	84.2%	10.5%	54.5%	16.9%
Avg							8.5%	48.1%	19.8%
Total Avg							3.0%	41.5%	19.9%

Table 2: Results of DecQN compared with DAPP, RP and GP on small instances

We now discuss the performance of DecQN on instances with Moderate, High and Very High customer density. The test set is obtained by sampling 500 customer realizations and 500 demand realizations for each instance $i \in I$ with Moderate, High and Very High customer density, resulting in 250,000 scenarios. The aggregated results are reported in Table 3, where the first four columns indicate the characteristics of the instance. The expected total demand for each instance is reported in column $\mathbb{E} \sum d_c$. The results of DecQN, along with the results of the two benchmarks, are reported in columns DecQN, RP, and GP, respectively. DecQN outperforms RP and GR by 70.4% and 9.3%, on average. The significant improvement

Ψ_{n_z}	Q	m	L	$\mathbb{E} \sum d_c$	DecQN	% $\mathbb{E} \sum d_c$	RP	GP	%RP	%GP
Moderate	25	3	221.5	230	159.1	69.2%	99.9	143.0	59.2%	11.3%
	50				193.1	83.9%	120.6	171.4	60.2%	12.7%
	75				210.1	91.4%	128.9	192.4	63.0%	9.2%
Avg									60.8%	11.1%
High	25	7	195.5	530	360.9	68.1%	217.9	321.5	65.6%	12.3%
	50				452.7	85.4%	264.5	417.9	71.1%	8.3%
	75				501.2	94.6%	269.6	460.0	85.9%	8.9%
Avg									74.2%	9.8%
Very High	25	11	187.3	830	552.5	66.6%	334.0	502.5	65.4%	9.9%
	50				703.0	84.7%	402.8	664.8	74.6%	5.8%
	75				778.7	93.8%	412.2	738.2	88.9%	5.5%
Avg									76.3%	7.0%
Total Avg									70.4%	9.3%

Table 3: Results of DecQN compared with RP and GP

over RP demonstrates the effect of the learning. According to Table 3, %GP falls from 11.1% to 7.0%, as the customer density increases. As previously stated, we argue that, as the customer density increases, the instance becomes relatively simpler for GP. To demonstrate this behavior in our results, we analyze the sensitivity of GP to variations in customer density. To this purpose, we normalize the demand served by GP by $\mathbb{E} \sum d_c$. Notice that the value of $\mathbb{E} \sum d_c$ solely depends on the level of Ψ_{n_z} ; hence, $\% \frac{\text{GP}}{\mathbb{E} \sum d_c}$ gives us a normalized measure that can be used to assess the performance of GP with respect to variations in customer density. This value can also be viewed as the ratio of demands served by GP. The right side of Table 4

reports the average values of $\% \frac{GP}{\sum d_c}$. We observe that, as the customer density rises, GP serves a larger ratio of demands. Specifically, the average ratio of demands served by GP increases from 73.4% to 76.5% when the customer density increases from Moderate to Very High. One intuitive explanation for this is that, as customers in the service area become denser, the problem for each vehicle will be more of a customer selection problem rather than a routing problem, where a long-term collective reward plays a decisive role. As a result, GP, which ignores the routing component, performs better on more densely populated service area. The left side of Table 4 reports average values of $\% \frac{DecQN}{\sum d_c}$. We observe that the performance of the DecQN remains approximately constant as the customer density varies. In particular, the value of $\% \frac{DecQN}{\sum d_c}$, averaged across different values of Q , remains around $\approx 82\%$ for each level of customer density. This finding is noteworthy because it implies that increases in the problem size due to higher customer density Ψ_{n_z} , do not deteriorate the performance of DecQN. Additionally, in line with the earlier discussion, we may attribute this result to the fact that, unlike GP, DecQN accounts for routing.

$\% \frac{DecQN}{\sum d_c}$		Q				$\% \frac{GP}{\sum d_c}$		Q			
		25	50	75	Avg			25	50	75	Avg
Ψ_{n_z}	Moderate	69.2%	83.9%	91.4%	81.5%	Ψ_{n_z}	Moderate	62.2%	74.5%	83.6%	73.4%
	High	68.1%	85.4%	94.6%	82.7%		High	60.7%	78.9%	86.8%	75.4%
	Very High	66.6%	84.7%	93.8%	81.7%		Very High	60.6%	80.1%	88.9%	76.5%
Avg		67.9%	84.7%	93.3%	81.9%	Avg		61.1%	77.8%	86.5%	75.1%

Table 4: The ratio of demands served by DecQN and GP

Finally, Table 3 shows that the %GP is usually higher when Q is smaller. For example, considering instances with Very High customer density, the %GP declines from 9.9% to 5.5% when the vehicle capacity increases from 25 to 75. A possible reason for this result is that, according to Table 4, as Q increases, the percentage of demands served by DecQN and GP increases to serve almost all demands. Thus there is a lower margin of improvement in higher vehicle capacities, which reduces the potential difference between their performances.

6.2 Performance of DecQN in VRPSD

The VRPSD can be seen as a particular version of the VRP-VCS, where the set of customers, including their locations and expected demands, is known in advance. Given that the purpose of DecQN is to handle variable customer sets, it does not assume the knowledge of customer locations, nor is designed to take advantage of such information. However, we now show that DecQN can compete with the solution method proposed by Goodson, Thomas, and Ohlmann (2016), which is the best-performing benchmark specialized for VRPSDs with duration limits and multiple vehicles.

In Section 6.2.1, we define the instance set and describe the scenario generation procedure. For each instance, we train DecQN over 3 million scenarios. Similar to the previous section, we decay the exploration and the learning rates linearly from 1.0 and 10^{-3} to 0.1 and 10^{-4} in the first 300K and 1.5 million trials. We describe the benchmark in Section 6.2.2 and discuss the results in Section 6.2.3.

6.2.1 VRPSD Instances

The VRPSD, as a particular version of the VRP-VCS, assumes that the number of customers, their locations and their expected demands are given in advance. Therefore, the distribution functions $\Psi_{n_z}, \Psi_l, \Psi_{\bar{d}}$ do not play a role in this section. The remaining instance-defining components $(\mathcal{A}, \Psi_{\bar{d}}, m, Q, L)$ are determined according to the procedure used in Goodson, Thomas, and Ohlmann (2016), which is described in Appendix B.1.2.

Goodson, Thomas, and Ohlmann (2016) conduct experiments on 216 instances. However, testing the DecQN on the full set of instances is time-consuming and beyond the scope of this paper. Therefore, we choose a subset of relatively challenging instances. In particular, we focus on instances with $n = 75$ constructed from R101 Solomon instances. In these instances, the number of vehicles m is 11. We identify a

VRPSD instance $i \in I$ as (L, Q, U) with $L \in \mathcal{L}$, $Q \in \mathcal{Q}$, and $U \in \mathcal{U}$. We denote U as the stochastic variability of the demands $\Psi_{\hat{d}}$. We define \mathcal{L} , \mathcal{Q} , and \mathcal{U} as follows: $\mathcal{L} = \{\text{Short, Medium, Long}\}$, $\mathcal{Q} = \{25, 50, 75\}$, and $\mathcal{U} = \{\text{Low, Moderate, High}\}$. A total of 27 instances are tested.

6.2.2 Benchmarks

Goodson, Thomas, and Ohlmann (2016) proposed a rollout algorithm (RA) based on a restocking fixed-route policy. The RA is a form of forward-dynamic programming that can be viewed as a one-step policy iteration (Bertsekas 2013). At each decision epoch, they generate a set of fixed routes using a local search heuristic. Each fixed route is then evaluated using a reward-to-go function for a set of sample demand realizations. Finally, the fixed route with the highest reward-to-go is selected, and the next move on that route is chosen. To account for preemptive actions for instances with up to 25 customers, they solve an auxiliary dynamic program to evaluate the reward-to-go of following a fixed route with and without performing a restocking move. For instances with more than 25 customers, they proposed a dynamic decomposition method to partition customers between vehicles, enabling them to handle instances of up to 100 customers. Goodson, Thomas, and Ohlmann (2016) obtain the initial fixed route by solving the VRPSD using a Simulated Annealing algorithm. They showed that the high-quality initial fixed route plays a vital role. According to their findings, starting with a high-quality initial solution outperforms the case of starting with a low-quality (randomly produced) fixed route by an average of 11.2%. We refer to this benchmark policy as GHQ when the algorithm starts with a high-quality fixed route, and refer to it as GLQ when the algorithm starts with a low-quality fixed route.

6.2.3 Results and Discussion

The test set $\hat{I}(i)$ is obtained by sampling 500 demand realizations for each instance $i \in I$. The performance of our method is then compared with two benchmark policies, GLQ and GHQ. GLQ is analogous to our method in that, like DecQN, it does not need computing an initial route for each instance. On the other hand, GHQ necessitates the computation of a high-quality initial route for each $i \in I$ instance.

The comparison is summarized in Table 5. In this table, the first three columns indicate the characteristics of the instance. The duration limits S, M, and L, respectively, refer to Short, Medium, and Long. The values L, M, and H for the stochastic variability are abbreviations for Low, Moderate, and High, respectively. The total served demand by DecQN averaged over 500 realizations ($\hat{I}(i)$) for each instance $i \in I$ is reported as DecQN. Column $(\% \mathbb{E} \sum d_c)$ shows the ratio of demands that DecQN serves. Note that the total expected demand for each instance is 1079. The results of the benchmarks are shown in columns GLQ and GHQ. Columns %GLQ and %GHQ display the percentage improvement of our method over GLQ and GHQ.

Overall, results show that DecQN outperforms the GLQ on average by 4.6%, while GHQ outperforms DecQN by 1.6%. To facilitate the discussion, the results are aggregated with respect to L, Q , and U in Table 6. Comparing the percentage improvements, averaged for each level of duration limit, demonstrates the considerable impact of the duration limit on the gap between our method and two benchmarks. We observe that, as the duration limit becomes longer, the gap between the performance of methods is less pronounced. In particular, when the duration limit changes from Short to Long, the absolute average value of %GLQ and %GHQ fall from 9.2% and 3.1% to 1.4% and 0.3%, respectively. This reduction in the gap may be explained by observing that, when the duration limit increases, it become less binding, and all methods are able to serve almost all demands. This logic is also supported by results reported in the fifth column $(\% \mathbb{E} \sum d_c)$ of Table 5. The DecQN serves almost all demands (at least 90.0%, except for instances with $(L, Q) = (\text{Medium}, 25)$) when the duration limit is Medium or Long. We now assess the impact of the vehicle capacity. Table 6 shows that the average %GHQ declines when vehicle capacity is reduced, whereas DecQN widens the gap with GLQ. Since smaller vehicle capacities imply a larger number of restocking operations, this result may be interpreted as a sign that DecQN successfully handles preventative restocking operations.

Regarding the impact of the stochastic variability, Table 6 shows an overall reduction in the absolute average gaps (%GLQ and %GHQ) as U increases from Low to High. This behavior can be explained by

<i>L</i>	<i>Q</i>	<i>U</i>	DecQN	$\% \mathbb{E} \sum d_c$	GLQ	GHQ	%GLQ	%GHQ
S	25	L	580.6	53.8%	534.6	595.9	8.6%	-2.6%
		M	556.3	51.6%	475.1	566.6	17.1%	-1.8%
		H	534.0	49.5%	479.8	527.5	11.3%	1.2%
	50	L	799.7	74.1%	738.3	834.0	8.3%	-4.1%
		M	781.0	72.4%	718.5	794.7	8.7%	-1.7%
		H	751.0	69.6%	704.9	760.4	6.5%	-1.2%
	75	L	934.0	86.6%	848.7	1011.4	10.1%	-7.7%
		M	902.4	83.6%	845.2	966.2	6.8%	-6.6%
		H	885.4	82.1%	839.3	913.5	5.5%	-3.1%
M	25	L	825.8	76.5%	785.6	842.9	5.1%	-2.0%
		M	800.3	74.2%	778.2	808.6	2.9%	-1.0%
		H	770.7	71.4%	747.3	776.2	3.1%	-0.7%
	50	L	1054.8	97.8%	1019.2	1077.5	3.5%	-2.1%
		M	1035.8	96.0%	1002.8	1067.0	3.3%	-2.9%
		H	1023.8	94.9%	977.1	1043.6	4.8%	-1.9%
	75	L	1074.5	99.6%	1058.3	1078.4	1.5%	-0.4%
		M	1072.8	99.4%	1052.1	1077.2	2.0%	-0.4%
		H	1069.7	99.1%	1044.4	1075.3	2.4%	-0.5%
L	25	L	1004.1	93.1%	974.4	1039.0	3.1%	-3.4%
		M	984.5	91.2%	959.9	998.6	2.6%	-1.4%
		H	971.3	90.0%	940.3	968.0	3.3%	0.3%
	50	L	1078.7	100.0%	1078.3	1078.3	0.0%	0.0%
		M	1080.3	100.1%	1076.3	1076.9	0.4%	0.3%
		H	1081.4	100.2%	1072.3	1075.3	0.9%	0.6%
	75	L	1079.7	100.1%	1078.4	1078.4	0.1%	0.1%
		M	1081.8	100.3%	1077.4	1077.5	0.4%	0.4%
		H	1082.7	100.3%	1075.5	1075.6	0.7%	0.7%
Avg							4.6%	-1.6%

Table 5: Results of DecQN compared with Goodson, Thomas, and Ohlmann (2016)

Avg Imp.	<i>L</i>			<i>Q</i>			<i>U</i>			Total
	S	M	L	25	50	75	L	M	H	
%GLQ	9.2%	3.2%	1.4%	6.3%	4.0%	3.3%	4.5%	4.9%	4.3%	4.6%
%GHQ	-3.1%	-1.4%	-0.3%	-1.3%	-1.5%	-1.9%	-2.5%	-1.7%	-0.5%	-1.6%

Table 6: Average improvement of DecQN over GLQ and GHQ with respect to *L*, *Q*, and *U*

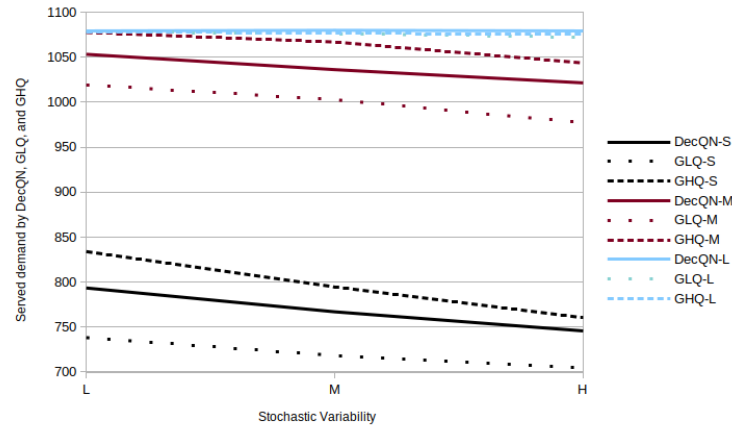


Figure 2: Performance of DecQN, GLQ, and GHQ with respect to the stochastic variability

looking into the difference between GLQ and GHQ. Figure 2 illustrates the trend of served demands by DecQN, GLQ, and GHQ, when the capacity is 50, in different levels of duration limit with respect to changes in stochastic variability. In this figure, results for different duration limits are identified by an indication appended to the policy name. For example, DecQN-S refers to the results of DecQN in instances with a Short duration limit. As shown in this figure, the increase in U narrows the gap between GLQ and GHQ when the duration limit is Low. This finding implies that as the stochastic variability increases, having a high-quality initial solution becomes less important. This figure also explains why the gap between GLQ and GHQ, and consequently %GLQ and %GHQ, do not follow a descending trend (as in instances with Short L) when U rises. The amount of served demands in instances with Medium and Long duration limit are very close to the total expected demand (i.e., 1079), making the performance of policies bounded. Hence the gap between GLQ and GHQ cannot follow the same trend as in instances with a Short duration limit. Another important finding is that while the performance of GHQ, when U increases from Low to High in instances with Short L , drops by 10.0% (from 595.9, 834.0, and 1011.4 to 527.5, 760.4, and 913.5, respectively for Small, Medium, and Large Q), the performance of our DecQN decreases only by 6.4% (from 580.6, 799.7, and 934.0 to 534.0, 751.0, and 885.4, respectively for Small, Medium, and Large Q). It can be deduced that our method is relatively better at dealing with stochastic variability than GHQ.

A last comment concerns the computing times. Given that GLQ starts from a random set of routes, the initialization time is negligible. Conversely, GHQ necessitates the computation of a high-quality initial route for each instance $i \in I$. The computing times for establishing initial routes are not reported in Goodson, Thomas, and Ohlmann (2016). However, results shared with us by the authors, we conclude that the average CPU time dedicated to obtaining high-quality initial solutions for instances with 75 customers was 25,466 seconds (≈ 7 hours). In comparison, our method, once trained for 24 to 36 hours, can be used with no further computation as long as the instance (including the associated distribution functions and parameters such as L, Q, U) remains the same. Therefore, we can roughly claim that using our method for more than five ($\approx \frac{36}{7}$) operating days is computationally advantageous over the GHQ.

Summarizing, we observed that DecQN and GLQ are analogous in the sense they both start with a random initial policy and solution. Results showed that the DecQN method could outperform GLQ by 4.6% on average. On the other hand, the average gap between DecQN and GHQ, where a high-quality initial solution is required, is -1.6%. However, results showed that the advantages of starting from a high-quality initial solution become less pronounced for higher values of stochastic variability. Furthermore, obtaining high-quality initial solutions is computationally expensive, and DecQN resulted computationally advantageous with respect to GHQ after five days of operations.

6.3 Generalized DecQN

The previous section showed that when DecQN is trained on VRPSD instances, it can compete with Goodson, Thomas, and Ohlmann (2016). However, it was necessary to train a new policy for each instance $i \in I$. In this experiment, we further explore the flexibility of the DecQN in terms of its generalization capabilities. Specifically, we investigate the possibility to train one DecQN model to solve a group of VRPSD instances I' , where $I' \subset I$. This also has some practical advantages, as it would be beneficial for a manager to apply the same policy regardless of, for example, the duration limit.

We use the same instances described in Section 6.2.1, but we restrict our analysis to instances with $Q = 50$ (i.e., $I = \mathcal{L} \times \{50\} \times \mathcal{U}$). We carry out the experiment in three steps. In the first step, we aggregate instances with respect to the duration limit L . Accordingly, we train three policies, each for a $U \in \mathcal{U}$. More specifically, in instances aggregated over L , the duration limit follows a uniform distribution function to pick a value from \mathcal{L} . Similarly, we generalize the method over the stochastic variability U in the next step. In the last step, we generalize the DecQN over both components. In this setting, a single policy is trained to solve all nine instances. To provide enough information to DecQN, we append the value of the component on which we are aggregating to the observation representation. For example, when aggregating over the duration limit, we pass L as an extra component into Equation (21), resulting in $o_{k,\bar{v}} = [F_k|H_k|G_k|t_k|L]$.

Once we obtain a policy, we test it on all instances considered in the training phase. As in the previous experiments, the training and testing realization sets are disjoint. For the first step, Table 7 summarizes the results of the trained policies (DecQN_L) and compares them with those trained in Section 6.2 (DecQN) and the two benchmark policies, GLQ and GHQ. Detailed computational results are reported in Table 12, in Appendix C. Table 7 reports the improvement percentage of the generalized policy over the benchmarks, averaged for each instance characteristic. Results show that the aggregation over the duration limit performs on average 2.3% and 3.7% worse than the individual policies (DecQN) and the GHQ, respectively. However, it still outperforms the GLQ by 1.6%. It can also be seen that the gap between DecQN_L and DecQN decreases when the duration limit gets longer (i.e., from -4.6% to -0.1%). Also, the aggregation works relatively better in higher stochastic variability.

Avg Imp.	L			U			Total
	S	M	L	L	M	H	
%DecQN	-4.6%	-2.2%	-0.1%	-2.3%	-2.5%	-2.0%	-2.3%
%GLQ	2.9%	1.6%	0.3%	1.5%	1.4%	1.9%	1.6%
%GHQ	-6.8%	-4.4%	0.2%	-4.3%	-3.9%	-2.8%	-3.7%

Table 7: Average improvement of DecQN_L over DecQN, GLQ, and GHQ

Table 8 reports the results of the second step (DecQN_U), where instances are aggregated with respect to the stochastic variability. Detailed results are provided in Table 13 in Appendix C. Similar to the previous analysis, we compare the results with the individual (DecQN) and benchmark (GLQ and GHQ) policies. Results show that our method can handle a broader range of instances at the expense of performing on average 0.7% worse than the individual policies. Interestingly, it can be seen that the generalized DecQN performs as well as the individual policies in instances with Medium and Long duration limits. Although the generalized model has a gap of -2.2% with the GHQ, it still considerably outperforms the GLQ (3.2%).

Avg Imp.	L			U			Total
	S	M	L	L	M	H	
%DecQN	-2.2%	0.0%	0.0%	-1.2%	-0.8%	-0.3%	-0.7%
%GLQ	5.4%	3.9%	0.4%	2.7%	3.3%	3.8%	3.2%
%GHQ	-4.5%	-2.3%	0.3%	-3.2%	-2.2%	-1.1%	-2.2%

Table 8: Average improvement of DecQN_U over DecQN, GLQ, and GHQ

Finally, Table 9 reports the performance of the single policy trained on all nine instances (DecQN_{All}). Detailed results are provided in Table 14 in Appendix C. Similar to Tables 7 and 8, we compare the performance of the generalized DecQN with the individual and benchmark policies. Results show that DecQN_{All}

is able to solve a set of instances with varying values of L and U at the expense of a 2.1% reduction of the performance quality. Confronting these results with those obtained in Tables 7 and 8, we can deduce that most of the performance deterioration comes from the generalization over the time limit dimension L . This experiment also shows that, if suitably trained, the proposed algorithm can be adapted to handle problems with varying features such as, for example, different duration limits.

Avg Imp.	L			U			Total
	S	M	L	L	M	H	
%DecQN	-4.3%	-1.9%	-0.2%	-2.7%	-2.2%	-1.4%	-2.1%
%GLQ	3.2%	1.9%	0.2%	1.0%	1.8%	2.5%	1.8%
%GHQ	-6.6%	-4.2%	0.1%	-4.7%	-3.6%	-2.3%	-3.5%

Table 9: Average improvement of DecQN_{All} over DecQN, GLQ, and GHQ

7 Conclusions

Motivated by a distribution planning problem arising in domestic donor collection services, we introduced the VRP-VCSD. In this problem, customer locations and demands are stochastic, and a fleet of capacitated vehicles must complete the service within a specified time limit. The goal is to maximize the total served demand. We provided two problem formulations based on Markov Decision Process. The first follows a traditional centralized decision-making perspective, while the second models a partially decentralized decision-making framework where vehicles autonomously establish their routes according to the observed state of the system. This second formulation enabled us to drastically reduce the dimension of the state and the action spaces, thus resulting in a more tractable problem. Variable-sized stochastic customer sets have been addressed via a heatmap-style representation of the customer demands. This approach, in particular, partitions the stochastic customers geographically and encodes them as a fixed-size vector. We then solved the resulting problem by a Q-learning algorithm. For this purpose, we developed a two-layer artificial neural network to approximate state-action Q factors. Computational results showed that our method significantly outperforms three benchmarks policies (DAPP, RP, and GP). Although DAPP provided better bounds than the other benchmarks, it could only handle instances with up to 15 customers. Furthermore, we evaluated the DecQN on the VRPSD, which is a particular case of VRP-VCSD, and showed that our method could compete with the state-of-the-art solution method specialized for that problem. As a further investigation into the capabilities of our framework, we tested and showed that the DecQN could be generalized over several problem components, such as the stochastic variability of demands. Finally, as shown in Appendix D, the obtained policies and value functions can be easily employed as a base policy and a reward-to-go estimator in on-line rollout methods.

As DecQN can efficiently handle problems with stochastic customer sets, it is promising to investigate how it could be extended to tackle dynamic versions of the VRP, where customers arise dynamically during the execution period. Another potential avenue is to investigate how the partially decentralized approach can be applied to other SVRPs, to handle, for example, stochastic travel time.

References

- 211 of Greater Montréal, 2022 *Where can I donate?* Accessed 7 Mar 2022, <https://www.211qc.ca/en/material-assistance-and-housing/used-articles-donation>.
- Bertsekas DP, 2013 *Rollout algorithms for discrete optimization: A survey*. Pardalos PM, Du DZ, Graham RL, eds., *Handbook of Combinatorial Optimization*, 2989–3013 (New York, NY: Springer New York).
- Big Brothers Big Sisters, 2022 *Home Pick-up*. Accessed 7 Mar 2022, <https://gfgsmtl.qc.ca/en/donate-clothes/home-pick-up/>.
- Bono G, Dibangoye JS, Simonin O, et al., 2020 *Solving multi-agent routing problems using deep attention mechanisms*. *IEEE Transactions on Intelligent Transportation Systems* 1–10.
- Brinkmann J, Ulmer MW, Mattfeld DC, 2019a *Dynamic lookahead policies for stochastic-dynamic inventory routing in bike sharing systems*. *Computers & Operations Research* 106:260–279.

- Brinkmann J, Ulmer MW, Mattfeld DC, 2019b *The multi-vehicle stochastic-dynamic inventory routing problem for bike sharing systems. Business Research 2019 13:1 13(1):69–92.*
- Chen X, Ulmer MW, Thomas BW, 2022 *Deep Q-learning for same-day delivery with vehicles and drones. European Journal of Operational Research 298(3):939–952.*
- Chen Y, Qian Y, Yao Y, et al., 2019 *A case study in dynamic courier dispatching system. In Proceedings of the 18th International Conference on Autonomous Agents and MultiAgent Systems, 1395–1403.*
- Curran A, Williams I, 2010 *The role of furniture and appliance re-use organisations in England and Wales. Resources, Conservation and Recycling 54(10):692–703.*
- EEA, 2022 *Reaching 2030’s residual municipal waste target — why recycling is not enough. European Environment Agency 1–14.*
- Erera AL, Morales JC, Savelsbergh M, 2010 *The vehicle routing problem with stochastic demand and duration constraints. Transportation Science 44(4):474–492.*
- Fan J, Wang X, Ning H, 2006 *A multiple vehicles routing problem algorithm with stochastic demand. 6th World Congress on Intelligent Control and Automation, 1688–1692 (IEEE).*
- Fortuna LM, Diyamandoglu V, 2017 *Optimization of greenhouse gas emissions in second-hand consumer product recovery through reuse platforms. Waste Management 66:178–189.*
- Gendreau M, Laporte G, Séguin R, 1995 *An exact algorithm for the vehicle routing problem with stochastic demands and customers. Transportation Science 29(2):143–155.*
- Goodson JC, Ohlmann JW, Thomas BW, 2013 *Rollout policies for dynamic solutions to the multivehicle routing problem with stochastic demand and duration limits. Operations Research 61(1):138–154.*
- Goodson JC, Thomas BW, Ohlmann JW, 2016 *Restocking-based rollout policies for the vehicle routing problem with stochastic demand and duration limits. Transportation Science 50(2):591–607.*
- Gu F, Zhang W, Guo J, et al., 2019 *Exploring “Internet+Recycling”: Mass balance and life cycle assessment of a waste management system associated with a mobile application. Science of The Total Environment 649:172–185.*
- Joe W, Lau HC, 2020 *Deep reinforcement learning approach to solve dynamic vehicle routing problem with stochastic customers. Proceedings of the international conference on automated planning and scheduling, 394–402.*
- Kaza S, Yao LC, Bhada-Tata P, et al., 2018 *What a waste 2.0: A global snapshot of solid waste management to 2050 (Washington, DC: World Bank).*
- Kingma DP, Ba J, 2014 *Adam: A method for stochastic optimization. 3rd International Conference on Learning Representations, ICLR 2015 (International Conference on Learning Representations, ICLR).*
- Kullman ND, Cousineau M, Goodson JC, et al., 2021 *Dynamic ride-hailing with electric vehicles. Transportation Science In press.*
- Li J, Ma Y, Gao R, et al., 2021a *Deep reinforcement learning for solving the heterogeneous capacitated vehicle routing problem. IEEE Transactions on Cybernetics 1–14.*
- Li M, Qin Z, Jiao Y, et al., 2019 *Efficient ridesharing order dispatching with mean field multi-agent reinforcement learning. The WWW Conference, 983–994 (New York, NY, USA: ACM).*
- Li X, Luo W, Yuan M, et al., 2021b *Learning to optimize industry-scale dynamic pickup and delivery problems. Proceedings - International Conference on Data Engineering, 2511–2522 (IEEE).*
- Lin B, Ghaddar B, Nathwani J, 2021 *Deep reinforcement learning for the electric vehicle routing problem with time windows. IEEE Transactions on Intelligent Transportation Systems 1–11.*
- Louveaux FV, Salazar-González JJ, 2018 *Exact approach for the vehicle routing problem with stochastic demands and preventive returns. Transportation Science 52(6):1463–1478.*
- Maxwell MS, Restrepo M, Henderson SG, Topaloglu H, 2010 *Approximate dynamic programming for ambulance redeployment. INFORMS Journal on Computing 22(2):266–281.*
- Mendoza JE, Rousseau LM, Villegas JG, 2016 *A hybrid metaheuristic for the vehicle routing problem with stochastic demand and duration constraints. Journal of Heuristics 22(4):539–566.*
- Mnih V, Kavukcuoglu K, Silver D, Rusu AA, Veness J, et al., 2015 *Human-level control through deep reinforcement learning. Nature 518(7540):529–533.*
- Nazari M, Oroojlooy A, Takáč M, et al., 2018 *Deep reinforcement learning for solving the vehicle routing problem. Advances in Neural Information Processing Systems 31:9839–9849.*
- Novoa C, Storer R, 2009 *An approximate dynamic programming approach for the vehicle routing problem with stochastic demands. European Journal of Operational Research 196(2):509–515.*

- Oda T, Joe-Wong C, 2018 *Movi: A model-free approach to dynamic fleet management*. *IEEE INFOCOM 2018-IEEE Conference on Computer Communications*, 2708–2716 (IEEE).
- OroojlooyJadid A, Hajinezhad D, 2019 *A review of cooperative multi-agent deep reinforcement learning*. *arXiv preprint arXiv:1908.03963* .
- Oyola J, Arntzen H, Woodruff DL, 2017 *The stochastic vehicle routing problem, a literature review, Part II: solution methods*. *EURO Journal on Transportation and Logistics* 6(4):349–388.
- Oyola J, Arntzen H, Woodruff DL, 2018 *The stochastic vehicle routing problem, a literature review, part I: models*. *EURO Journal on Transportation and Logistics* 7(3):193–221.
- Peng B, Wang J, et al., 2020 *A deep reinforcement learning algorithm using dynamic attention for vehicle routing problems*. Li K, et al., eds., *AI Algorithms and Applications*, 636–650 (Springer, Singapore).
- Powell WB, 2011 *Approximate dynamic programming*. Wiley Series in Probability and Statistics (Hoboken, NJ, USA: John Wiley & Sons, Inc.).
- Ranjbari M, Saidani M, S Esfandabadi Z, et al., 2021 *Two decades of research on waste management in the circular economy: Insights from bibliometric, text mining, and content analyses*. *Journal of Cleaner Production* 314:128009.
- Ritzinger U, Puchinger J, Hartl RF, 2016 *A survey on dynamic and stochastic vehicle routing problems*. *International Journal of Production Research* 54(1):215–231.
- Rosu D, Aleman DM, Beck JC, et al., 2017 *Knowledge-Based provision of goods and services for people with social needs: Towards a virtual marketplace*. *AAAI Workshop*, 36–42.
- Sandin G, Peters GM, 2018 *Environmental impact of textile reuse and recycling – A review*. *Journal of Cleaner Production* 184:353–365.
- Secomandi N, 2001 *A rollout policy for the vehicle routing problem with stochastic demands*. *Operations Research* 49(5):796–802.
- Shirvanimoghaddam K, Motamed B, Ramakrishna S, et al., 2020 *Death by waste: Fashion and textile circular economy case*. *Science of The Total Environment* 718:137317.
- Soeffker N, Ulmer MW, Mattfeld DC, 2022 *Stochastic dynamic vehicle routing in the light of prescriptive analytics: A review*. *European Journal of Operational Research* 298(3):801–820.
- Solomon MM, 1987 *Algorithms for the vehicle routing and scheduling problems with time window constraints*. *Operations Research* 35(2):254–265.
- Ulmer MW, 2020 *Dynamic pricing and routing for same-day delivery*. *Transportation Science* 54(4):1016–1033.
- Ulmer MW, Goodson JC, Mattfeld DC, et al., 2017 *Offline-online approximate dynamic programming for dynamic vehicle routing with stochastic requests*. *Transportation Science* 53(1):1–35.
- Ulmer MW, Mattfeld DC, Köster F, 2018 *Budgeting time for dynamic vehicle routing with stochastic customer requests*. *Transportation Science* 52(1):20–37.
- UN, 2021 *The Sustainable Development Goals*. Accessed 30 Apr 2022, <https://sdgs.un.org/goals/goal12>.
- US EPA, 2019 *Durable goods: Product-specific data*. Accessed 25 Feb 2022, <https://www.epa.gov/facts-and-figures-about-materials-waste-and-recycling/durable-goods-product-specific-data>.
- Van Hasselt H, Guez A, Silver D, 2016 *Deep reinforcement learning with double Q-learning*. *Proceedings of the AAAI Conference on Artificial Intelligence*.
- Voccia SA, Campbell AM, Thomas BW, 2013 *The probabilistic traveling salesman problem with time windows*. *EURO Journal on Transportation and Logistics* 2(1-2):89–107.
- Watkins CJCH, Dayan P, 1992 *Q-learning*. *Machine Learning* 8(3-4):279–292.
- Zanjirani Farahani R, Asgari N, Van Wassenhove LN, 2021 *Fast Fashion, Charities, and the Circular Economy: Challenges for operations management*. *Production and Operations Management* 31(3):1089–1114.

A Algorithms

A.1 Q-learning algorithm

Q-learning is a model-free algorithm based on approximate value iteration in which an agent learns how to behave in order to maximize the collected reward through a sequence of interactions with the environment, resulting in a policy that satisfies Equation (26). More specifically, this method iteratively updates the value of making the action x_k in state s_k , known as the Q factor of that state-action pair ($Q(s_k, x_k)$). In fact, it is possible to rewrite the Bellman equation (defined in Equation (25)) in terms of Q factors as follows:

$$V(s_k) = \max_{x_k \in A(s_k)} Q(s_k, x_k), \quad (32)$$

where:

$$Q(s_k, x_k) = R(s_k, x_k, w) + \gamma \max_{x_{k+1} \in A(s_{k+1})} Q(s_{k+1}, x_{k+1}).$$

The reader is referred to (Powell 2011) for a complete overview of the algorithm. Algorithm 1 illustrates a generic Q-learning framework. To summarize, this algorithm simulates the problem for several trials (*Trials_MAX*) over different sample scenarios of stochastic components of the problem. The simulation follows the so-called ϵ -greedy policy, which enables random exploration of the action space. The level of exploration is typically larger in the initial phases of the algorithm when actions are mostly chosen randomly. As the algorithm proceeds, actions with higher estimated values are generally preferred. Q-learning exploits the interactions between the agent and the environment to update the Q values (the so-called *experiences*). An experience is defined as a tuple of (s_k, x_k, r_k, s_{k+1}) , describing interaction of the agent with the environment consisting of the agent observation of the state s_k , its action x_k , the received reward r_k (in VRP-VCSD, $r_k = R(s_k, x_k, w)$) and the observation of the next state s_{k+1} . For each state-action pair experienced, we estimate their Q value as $\hat{Q}(s_k, x_k)$ using the following equation:

$$\hat{Q}(s_k, x_k) = r_k + \gamma \max_{x_{k+1} \in A(s_{k+1})} Q(s_{k+1}, x_{k+1}), \quad (33)$$

where γ is the discount factor. Then, we update the $Q(s_k, x_k)$ according to the following equation:

$$Q(s_k, x_k) \leftarrow Q(s_k, x_k) + \alpha * [\hat{Q}(s_k, x_k) - Q(s_k, x_k)], \quad (34)$$

where α is the step size (learning rate).

Algorithm 1 returns a set of Q values that can be used as the decision policy. In particular, the optimal decision policy will be:

$$\pi^*(s_k) = \arg \max_{x_k \in A(s_k)} Q(s_k, x_k). \quad (35)$$

A.2 The DecQN

This section illustrates the pseudo code for our proposed DecQN algorithm.

Algorithm 1: Generic Q-learning Algorithm

```

Initialize: set Q values to 0
while trials < Trials.MAX do
  Choose a sample scenario  $w$ 
  Observe state  $s_0$ 
   $k \leftarrow 0$ , simulate  $\leftarrow$  True
  while simulate do
    Take action:  $x_k \leftarrow \begin{cases} \text{random action in } A(s_k) & \epsilon \\ \arg \max_{x' \in A(s_k)} Q(s_k, x') & 1 - \epsilon \end{cases}$ 

    Transit to  $s_{k+1} \leftarrow S^M(s_k, x_k, w_{k+1})$  and observe the reward  $r_k$ 

    Estimate and update new Q values:
    •  $\hat{Q}(s_k, x_k) \leftarrow \begin{cases} r_k & A(s_{k+1}) = \emptyset \\ r_k + \gamma \max_{x' \in A(s_{k+1})} Q(s_{k+1}, x') & \text{otherwise} \end{cases}$ 

    •  $Q(s_k, x_k) \leftarrow Q(s_k, x_k) + \alpha[\hat{Q}(s_k, x_k) - Q(s_k, x_k)]$ 

     $k \leftarrow k + 1$ 
    if  $A(s_k) = \emptyset$  then
      | simulate  $\leftarrow$  False
    end
  end
  Set trials = trials + 1
  Decay the exploration rate  $\epsilon$ 
end
return Q values
  
```

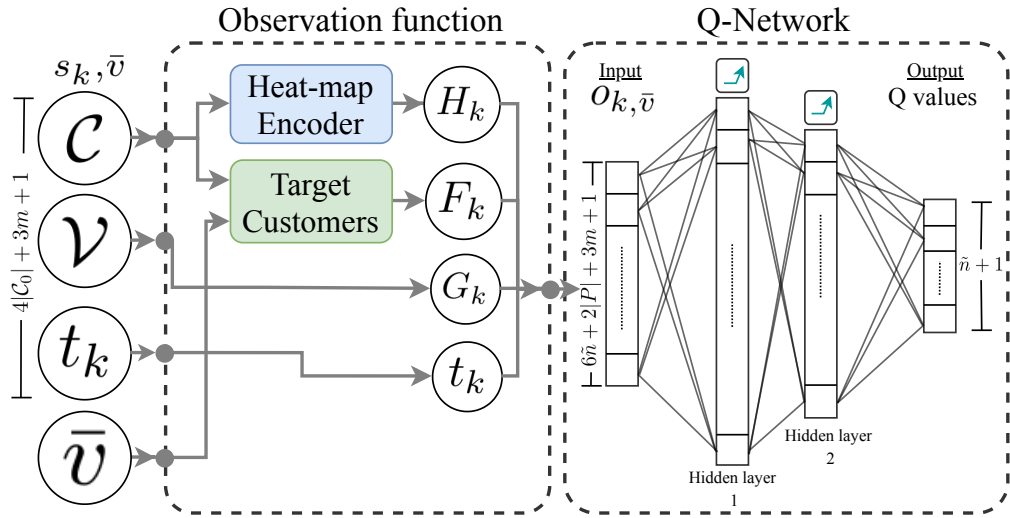


Figure 3: A schematic overview of DecQN

Algorithm 2: The DecQN

Initialize the Q-network and the target Q-network with random weights $\theta, \bar{\theta}$
 $B \leftarrow []$
while $trials < Trials_MAX$ **do**
 Choose a sample scenario w and observe a new set of customers C_0
 $t_0 \leftarrow 0, k \leftarrow 0, \bar{v}_{prev} \leftarrow \emptyset, Buff \leftarrow [\emptyset]_{v \in \mathcal{V}}$, and $simulate \leftarrow True$
while $simulate$ **do**
 $\bar{v} \leftarrow$ a random $v \in \bar{\mathcal{V}}$, where $\bar{\mathcal{V}} = \{v \in \mathcal{V} | a_v = t_k\}$
if $k > 0$ **then**
 Transit from s_{k-1}^x to s_k and observe the reward r
 $Buff[\bar{v}_{prev}] \leftarrow (s_{k-1}, \bar{v}_{prev}, x_{k-1}, s_k, \bar{v})$
if $Buff[\bar{v}] \neq \emptyset$ **then**
 $(s, v, x, s', v') \leftarrow Buff[\bar{v}]$
 Append (s, v, x, r, s', v') to B
end
end
 Observe $o_{k, \bar{v}} = O(s_k, \bar{v})$
 Take action: $x_k \leftarrow \begin{cases} \text{random action in } A(s_k, \bar{v}) & rand[0, 1] < \epsilon \\ \arg \max_{x'} Q(o_{k, \bar{v}}, x', \theta) & \text{otherwise} \end{cases}$
 Transit from s_k to s_k^x
if $rand[0, 1] < \beta_t$ **then**
 Estimate and update new Q values:

- Sample a batch of experiences \tilde{B} from B
- Compute the estimation

$$\hat{Q}(O(s, v), x, \theta) \leftarrow \begin{cases} r & A(s_k, v) = \{l_0\} \wedge l_v = l_0 \\ r + \gamma \max_{x'} Q(O(s', v'), x', \bar{\theta}) & \text{otherwise} \end{cases}, \forall (s, v, x, r, s', v') \in \tilde{B}$$
- Compute the loss function: $\Phi \leftarrow \mathbb{E}_{\tilde{B}} [Huber(Q(O(s, v), x, \theta) - \hat{Q}(O(s, v), x, \theta))]$
- Update the network weights θ : $\theta \leftarrow \theta - \alpha \nabla_{\theta} \Phi$

end
 $k \leftarrow k + 1$, and $\bar{v}_{prev} \leftarrow \bar{v}$
if $A(s_k, \bar{v}) = \emptyset \wedge l_v = l_0, \forall v \in \mathcal{V}$ **then**
 $simulate \leftarrow False$
end
end
 $trials \leftarrow trials + 1$
 Every β_d $trials$, $\bar{\theta} \leftarrow \theta$
 Decay the learning rate α and the exploration rate ϵ
end
return Q values

B Experimental setup

B.1 Instance generation

This section provides details on the methods used to generate the VRP-VCSD and VRPSD instances in our experiments.

B.1.1 VRP-VCSD instances

We consider a squared-shape service area \mathcal{A} of dimension 100×100 with a depot located at the center ($l_0 = (50, 50)$). Customers can potentially be located at any position inside the service area. However, in real-life applications, certain zones of the service area never generate requests, such as non-residential areas. Therefore, for a given service area partitioned into a set of 5×5 square-shaped zones \mathcal{Z} , we randomly pick a subset \mathcal{Z} of *active* zones, in which customers must be located. In our experiment, we consider 15 active zones out of 25 (i.e., 60% of the zones are active). Figure 4 shows the layout of the considered region.

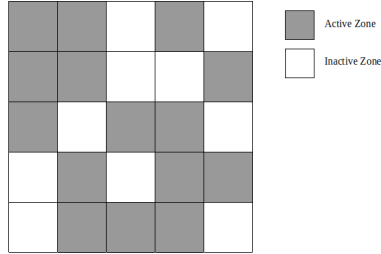


Figure 4: The layout of active zones

To generate the customer locations and demands, we make the assumption that active zones are homogeneous in the sense that the customer density Ψ_{n_z} and distributions Ψ_l , $\Psi_{\bar{d}}$, $\Psi_{\hat{d}}$ do not depend on the specific zone. The customer density Ψ_{n_z} specifies the probability distribution of the number n_z of requests for each active zone. We consider five possible levels of customer density $\mathcal{D} = \{\text{Very Low, Low, Moderate, High, Very High}\}$. In particular, n_z takes values $\{0, 1, 2\}$ for Very Low and Low with probabilities $\{0.5, 0.3, 0.16\}$ and $\{0.3, 0.3, 0.3\}$, respectively. For denser instances, it takes values $\{0, 1, 2, 3\}$ for Moderate, $\{2, 3, 4, 5\}$ for High, and $\{4, 5, 6, 7\}$ for Very High customer densities, with probabilities $\{0.1, 0.4, 0.4, 0.1\}$, respectively. The corresponding expected number of customers at each zone \bar{n}_z is $0.6, 1.0, 1.5, 3.5$, and 5.5 , respectively. The total expected number of customers \bar{n} for a given Ψ_{n_z} is calculated as $\bar{n} = \mathbb{E}[\sum_{z \in \mathcal{Z}} n_z] = |\mathcal{Z}| * \bar{n}_z$, resulting in 10, 15, 23, 53, and 83 customers for Very Low, Low, Moderate, High, and Very High customer density, respectively. Once n_z is sampled according to the distribution Ψ_{n_z} for each zone $z \in \mathcal{Z}$, the customer locations are generated following the distribution Ψ_l . In this experiment, we choose Ψ_l to be the uniform distribution function over (x,y)-coordinates inside a given zone. The above process allows us to sample the initial set of customers \mathcal{C}_0 .

Given a customer $c \in \mathcal{C}_0$, the expected demand \bar{d}_c and actual demand \hat{d}_c are sampled according to distributions $\Psi_{\bar{d}}$ and $\Psi_{\hat{d}}$, respectively. These distributions are chosen following the method proposed in Gendreau, Laporte, and Séguin (1995). In particular, $\Psi_{\bar{d}}$ is the discrete uniform distribution over the values $\{5, 10, 15\}$. Once the value \bar{d}_c has been sampled, the actual demands follow the distribution $\Psi_{\hat{d}}$ which is the discrete uniform distribution on values $\{\bar{d}_c - 5, \dots, \bar{d}_c, \dots, \bar{d}_c + 5\}$. In order to avoid the no-demands case when $\bar{d}_c = 5$, we use the discrete uniform distribution function on values $\{\bar{d}_c - 4, \dots, \bar{d}_c, \dots, \bar{d}_c + 4\}$.

We determine the number of vehicles m and the time limit L uniquely as functions of the distribution Ψ_{n_z} by linking them through the concept of the filling rate. The filling rate $f = \frac{\mathbb{E}[\sum_{c \in \mathcal{C}_0} \bar{d}_c]}{m * Q}$ indicates the portion of all demands that can be served by all vehicles without replenishment. In the equation above, $\mathbb{E}[\sum_{c \in \mathcal{C}_0} \bar{d}_c]$ is the expected total demand and can be approximated by $\bar{n}_z * |\mathcal{Z}| * \bar{d}$, where \bar{d} is the average expected demand of a customer. Since the distribution function $\Psi_{\bar{d}}$ assigns expected demands 5, 10, or 15 to customers uniformly (with a probability of $\frac{1}{3}$), the average expected demand of a customer (\bar{d}) will be equal to 10 ($\frac{5+10+15}{3}$) in all instances. By fixing the filling rate and the vehicle capacity to 1 and 75, respectively,

the number of vehicles for each level of customer density Ψ_{n_z} can then be obtained by the definition of the filling rate:

$$m = \left\lceil \frac{\mathbb{E}[\sum_{c \in \mathcal{C}_0} \bar{d}_c]}{f * Q} \right\rceil = \left\lceil \frac{\bar{n}_z * |\mathcal{Z}| * \bar{d}}{f * Q} \right\rceil = \left\lceil \frac{\bar{n}_z * 15 * 10}{1 * 75} \right\rceil = \lceil 2 * \bar{n}_z \rceil. \quad (36)$$

In this way, the number of required vehicles for each class of customer density is 2, 2, 3, 7, and 11, respectively. Notice that, according to the expression $\mathbb{E}[\sum_{c \in \mathcal{C}_0} \bar{d}_c]$, the expected total demand at each instance will be 100, 150, 230, 530, and 830 for Very Low, Low, Moderate, High and Very High customer density, respectively.

To determine the duration limit L for a given instance with the customer density distribution Ψ_{n_z} and its associated m , we use the average travel time of vehicles acquired by solving a set of 250,000 realizations of that instance via GP (described in Section 6.1.2). In this process, we assumed that $L = \infty$, $Q = 75$, and realizations are randomly sampled from distributions $\Psi_{n_z}, \Psi_l, \Psi_{\bar{d}}, \Psi_{\hat{d}}$. To make the duration limit constraining, we let the duration limit be the average travel time of all vehicles multiplied by 0.75. The resulting duration limits for Very Low, Low, Moderate, High and Very High customer densities are 143.71, 201.38, 221.47, 195.54, and 187.29, respectively. To complete the description of the instance generation, we need to determine the values Q . According to Equation (36), the number of vehicles m is determined such that when $Q = 75$, vehicles can serve the total expected demand without replenishing at the depot. Therefore, for a given duration limit, while using smaller capacities (< 75) may increase the frequency of restocking operations, which results in serving fewer customers in a limited time, considering larger vehicle capacities (> 75) may not necessarily affect the performance of vehicles. Therefore, in this experiment, we consider three possible values $\mathcal{Q} = \{25, 50, 75\}$.

To summarize, the instance set I is obtained by varying the customer density distribution function $\Psi_{n_z} \in \mathcal{D} = \{\text{Very Low, Low, Moderate, High, Very High}\}$ and the vehicle capacity $Q \in \mathcal{Q} = \{25, 50, 75\}$, resulting in 15 different instances. Fixing the customer density distribution also uniquely determines the number of vehicles m and the time limit L . The rest of the instance-defining elements, namely the service area \mathcal{A} and the distributions $\Psi_l, \Psi_{\bar{d}}, \Psi_{\hat{d}}$ are kept fixed throughout the experiment. In other words an instance in this experiment is completely identified by the pair (Ψ_{n_z}, Q) . Finally, realizations \hat{i} of an instance i are obtained by sampling from distributions $\Psi_{n_z}, \Psi_l, \Psi_{\bar{d}}, \Psi_{\hat{d}}$.

B.1.2 VRPSD instances

Goodson, Ohlmann, and Thomas (2013) used the *R101* and *C101* instances from Solomon (1987) and took the first n customers to generate the set \mathcal{C}_0 with $n = 25, 50, 75$, and 100. Concerning expected demands, the authors used the deterministic demands provided by the Solomon's instances. To determine the number of vehicles m and the duration limit L , the authors solved each instance as a classical VRP using a heuristic with a vehicle capacity of 100. The resulting number of routes determines m , while a set of three time limits are obtained by multiplying the length of the longest route by 0.75, 1.25, and 1.75, resulting in $\mathcal{L} = \{\text{Short, Medium, Long}\}$. The considered duration limits Short, Medium, and Long are 103.05, 171.75, and 240.45, respectively. They also varied the vehicle capacity Q to take a size in $\mathcal{Q} = \{25, 50, 75\}$.

Regarding the distribution functions of the customer demands, they characterized $\Psi_{\bar{d}}$ by an instance identifier U , denoted as the stochastic variability of the demands. The stochastic variability U may have a value in $\mathcal{U} = \{\text{Low, Moderate, High}\}$. In particular, $\Psi_{\bar{d}}$ takes the distribution function of $\{\bar{d}/2, \bar{d}, 3\bar{d}/2\}$ with probabilities (0.05, 0.9, 0.05) for Low, $\{0, \bar{d}/2, \bar{d}, 3\bar{d}/2, 2\bar{d}\}$ with probabilities (0.05, 0.15, 0.6, 0.15, 0.05) for Moderate, and $\{0, \bar{d}/2, \bar{d}, 3\bar{d}/2, 2\bar{d}\}$ with a uniform probability for High stochastic variability, respectively. For details, the reader may refer to Goodson, Thomas, and Ohlmann (2016). In consequence, the authors conduct experiments on 216 instances, comprised of eight different sets of customers (i.e., four levels for the number of customers $\{25, 50, 75, 100\} \times$ two classes of instances $\{\text{R101, C101}\}$). In particular, for each set of customers with the same locations and expected demands, they did tests on 27 distinct instances.

B.2 Hyper-parameters and computing facility

The hyper-parameters in Algorithm 2 have been set as follows. We consider a minibatch of 32 experiences ($|\hat{B}| = 32$) uniformly sampled from the replay memory with a size of 50000, where $\beta_t = 0.05$. We also

replace the target network every 1000 trials ($\beta_d = 1000$). For all experiments, we set the discount factor γ to 0.999 (Kullman et al. 2021). The hyper-parameters related to the maximum number of trials ($Trials_MAX$) and the decaying factor for the learning rate (α) and the exploration rate (ϵ) will be specified for each experiment later. All the procedures have been implemented in python and executed on 3.6 GHz Intel Xeon processors with 64 GB RAM (no GPUs are used).

B.3 Deterministic Formulation

In this section, we present a mathematical formulation for the deterministic version of the VRP-VCSD. Unlike DecQN, where both customers and demands are stochastic, this formulation assumes that the set of customers is known, and the actual demand is equal to the expected value. In order to provide an upper bound for the possible number of trips for a vehicle (E), we propose a heuristic algorithm, which is illustrated in Algorithm 3. This algorithm computes the total number of trips for a vehicle in the worst-case scenario when it visits customers one-per-trip from closest to farthest in terms of their distance to the depot. This strategy results in the highest number of trips.

Notation	Description
N	set of nodes, $N = \mathcal{C}_0 \cup \{0\}$. Node 0 represents the depot.
i, j	index of nodes in N
\mathcal{E}	set of trips for a vehicle, $e \in \mathcal{E}$, $\mathcal{E} = \{0, 1, \dots, E - 1\}$
E	an upper bound for the number of trips for a vehicle
M	a big number
x_i^{ve}	the amount of node i 's demand that is served by vehicle v in trip e
y_{ij}^{ve}	binary variable takes 1 if node j is immediately visited after node i by vehicle v in trip e
λ_i^{ve}	binary variable takes 1 if customer i is visited by vehicle v in trip e
q_i^{ve}	available capacity of vehicle v when it arrives at node i in trip e
t_i^{ve}	time at which the vehicle v arrives at node i in trip e
\underline{t}^{ve}	time at which the vehicle v leaves the depot for trip e

Table 10: Notations of the deterministic formulation

$$\max \quad \sum_{i \in N} \sum_{v \in \mathcal{V}} \sum_{e \in \mathcal{E}} x_i^{ve} \quad (37)$$

$$\text{s.t.} \quad \sum_{j \in N} y_{ij}^{ve} \leq 1; \quad \forall i \in N, v \in \mathcal{V}, e \in \mathcal{E} \quad (38)$$

$$\sum_{j \in N} y_{ji}^{ve} \leq 1; \quad \forall i \in N, v \in \mathcal{V}, e \in \mathcal{E} \quad (39)$$

$$y_{ii}^{ve} = 0; \quad \forall i \in N, v \in \mathcal{V}, e \in \mathcal{E} \quad (40)$$

$$\sum_{i \in N} y_{0i}^{ve} \leq \sum_{i \in N} \lambda_i^{ve}; \quad \forall v \in \mathcal{V}, e \in \mathcal{E} \quad (41)$$

$$\sum_{j \in N} y_{ji}^{ve} = \sum_{j \in N} y_{ij}^{ve} = \lambda_i^{ve}; \quad \forall i \in N, v \in \mathcal{V}, e \in \mathcal{E} \quad (42)$$

$$\sum_{i \in N} \sum_{j \in N} y_{ij}^{ve} \leq M \left(\sum_{i \in N} \sum_{j \in N} y_{ij}^{v, e-1} \right); \quad \forall v \in \mathcal{V}, e \in \mathcal{E} \setminus 0 \quad (43)$$

$$\sum_{i \in N} \lambda_i^{ve} \leq M \left(\sum_{i \in N} \lambda_i^{v, e-1} \right); \quad \forall v \in \mathcal{V}, e \in \mathcal{E} \setminus 0 \quad (44)$$

$$x_i^{ve} \leq M \lambda_i^{ve}; \quad \forall i \in N, v \in \mathcal{V}, e \in \mathcal{E} \quad (45)$$

$$x_0^{ve} = 0; \quad \forall v \in \mathcal{V}, e \in \mathcal{E} \quad (46)$$

$$\sum_{v \in \mathcal{V}} \sum_{e \in \mathcal{E}} x_i^{ve} \leq d_i; \quad \forall i \in N \quad (47)$$

$$x_i^{ve} \leq q_i^{ve}; \quad \forall i \in N, v \in \mathcal{V}, e \in \mathcal{E} \quad (48)$$

$$\sum_{i \in N} x_i^{ve} \leq Q; \quad \forall v \in \mathcal{V}, e \in \mathcal{E} \quad (49)$$

$$q_j^{ve} \leq Q + M(1 - y_{0j}^{ve}); \quad \forall j \in N, v \in \mathcal{V}, e \in \mathcal{E} \quad (50)$$

$$q_j^{ve} \geq Q - M(1 - y_{0j}^{ve}); \quad \forall j \in N, v \in \mathcal{V}, e \in \mathcal{E} \quad (51)$$

$$q_j^{ve} \leq (q_i^{ve} - x_i^{ve}) + M(1 - y_{ij}^{ve}); \quad \forall i, j \in N, v \in \mathcal{V}, e \in \mathcal{E} \quad (52)$$

$$q_j^{ve} \geq (q_i^{ve} - x_i^{ve}) - M(1 - y_{ij}^{ve}); \quad \forall i, j \in N, v \in \mathcal{V}, e \in \mathcal{E} \quad (53)$$

$$q_i^{ve} \leq M\lambda_i^{ve}; \quad \forall i \in N, v \in \mathcal{V}, e \in \mathcal{E} \quad (54)$$

$$\underline{t}^{v0} = 0; \quad \forall v \in \mathcal{V} \quad (55)$$

$$\underline{t}^{v,e+1} = \underline{t}^{ve} + \sum_{i \in N} \sum_{j \in N} \tau_{ij} y_{ij}^{ve}; \quad \forall v \in \mathcal{V}, e \in \mathcal{E} \setminus 0 \quad (56)$$

$$t_j^{ve} \geq \underline{t}^{ve} + \tau_{0j} - M(1 - y_{0j}^{ve}); \quad \forall j \in N, v \in \mathcal{V}, e \in \mathcal{E} \quad (57)$$

$$t_j^{ve} \geq t_i^{ve} + \tau_{ij} - M(1 - y_{ij}^{ve}); \quad \forall i, j \in N \setminus 0, v \in \mathcal{V}, e \in \mathcal{E} \quad (58)$$

$$t_j^{ve} \leq M\lambda_j^{ve}; \quad \forall j \in N, v \in \mathcal{V}, e \in \mathcal{E} \quad (59)$$

$$\underline{t}^{v,E-1} + \sum_{i \in N} \sum_{j \in N} \tau_{ij} y_{ij}^{v,E-1} \leq L; \quad \forall v \in \mathcal{V} \quad (60)$$

$$0 \leq x_i^{ve}, q_i^{ve} \leq Q, 0 \leq t_i^{ve}, \underline{t}^{ve} \leq L, y_{ij}^{ve}, \lambda_i^{ve} \in \{0, 1\}; \quad \forall i, j \in N, v \in \mathcal{V}, e \in \mathcal{E}$$

In this mathematical formulation, the objective function (37) maximizes the total amount of served demands. Constraints (38)–(40) ensure that each customer cannot be visited more than once on each trip. Constraint (41) implies that if a vehicle visits no customer during a trip, no traverse between nodes should be planned for that vehicle on that trip. On the other hand, constraint (42) states that if a customer is decided to be served, a route to visit that customer should be planned. Constraints (43) and (44) guarantee that trips of a vehicle should be planned consecutively. Constraints (45)–(49) restrict the amount a vehicle can serve when visiting a customer on a trip by customer’s demand and vehicle capacity. Constraints (50)–(54) are flow balance constraints. Lastly, constraints (55)–(60) keep track of operation time and restrict it by the given duration limit.

Algorithm 3: Compute an upper bound for the number of trips of a vehicle E

C is the set of customers in C_0 ordered such that $\tau_{0i} \leq \tau_{0j}, \forall i < j$;

$E \leftarrow 0, i \leftarrow 0, l \leftarrow 0$;

while $l \leq L$ **do**

if $l + \tau_{0i} + \tau_{i0} > L$ **then**

return E ;

else

$l \leftarrow l + \tau_{0i} + \tau_{i0}$;

$E \leftarrow E + 1$;

if $d_i \geq Q$ **then**

$d_i \leftarrow d_i - Q$;

else

$i \leftarrow i + 1$;

C Extended computational results

This section provides extended results of the first and third experiment. Note that row Avg reports averages over instances solved to optimality by DAPP.

D On-line-off-line DecQN

In the previous experiments, we investigated the performance of the trained Q-network as a policy. More specifically, for a given Q-network that provides Q values for observation-action pairs, the policy applied the

Ψ_{n_z}	Q	n	$\mathbb{E} \sum d_c$	DecQN	$\% \mathbb{E} \sum d_c$	Opt. gap	DAPP	RP	GP	%DAPP	%RP	%GP		
Very Low	25	12	125.0	74.6	59.7%	66.7%	-	53.3	55.5	-	40.0%	34.3%		
		8	85.0	81.1	95.4%	0.0%	75.4	58.3	56.6	7.6%	39.0%	43.2%		
		9	100.0	61.8	61.8%	0.0%	61.2	46.4	49.6	1.0%	33.0%	24.5%		
		11	115.0	75.0	65.2%	0.0%	76.6	51.2	52.2	-2.1%	46.6%	43.5%		
		10	90.0	65.5	72.7%	0.0%	61.0	49.1	56.0	7.3%	33.4%	16.9%		
		11	95.0	52.8	55.5%	0.0%	53.0	39.5	44.8	-0.4%	33.7%	17.8%		
		12	125.0	81.7	65.4%	38.9%	-	59.7	69.2	-	37.0%	18.1%		
		10	95.0	58.1	61.2%	0.0%	55.8	44.5	51.4	4.1%	30.6%	13.0%		
		9	115.0	74.0	64.4%	0.0%	73.5	61.4	60.2	0.7%	20.5%	22.9%		
		12	105.0	64.9	61.8%	24.0%	-	48.3	52.7	-	34.3%	23.1%		
											Avg	2.6%	33.8%	26%
		50	12	125.0	102.4	81.9%	0.0%	101.3	66.1	96.1	1.1%	55.0%	6.5%	
	8		85.0	84.8	99.8%	0.0%	77.6	69.7	81.5	9.3%	21.8%	4.1%		
	9		100.0	85.3	85.3%	0.0%	85.0	58.0	66.2	0.3%	47.1%	28.8%		
	11		115.0	89.9	78.2%	0.0%	89.0	61.1	64.1	1.1%	47.1%	40.2%		
	10		90.0	85.8	95.3%	0.0%	83.8	55.6	83.8	2.3%	54.4%	2.3%		
	11		95.0	65.3	68.8%	0.0%	65.3	46.6	59.7	0.0%	40.3%	9.4%		
	12		125.0	108.8	87.0%	0.0%	108.8	72.3	69.6	0.0%	50.4%	56.3%		
	10		95.0	74.5	78.5%	0.0%	74.5	50.5	74.5	0.0%	47.6%	0.0%		
	9		115.0	90.3	78.5%	0.0%	89.7	71.9	80.4	0.7%	25.6%	12.4%		
	12		105.0	85.8	81.7%	0.0%	88.5	56.0	88.5	-3.0%	53.3%	-3.0%		
										Avg	1.2%	44.3%	15.7%	
	Low		25	14	145.0	105.7	72.9%	26.1%	-	67.5	87.7	-	56.5%	20.5%
		14		125.0	81.5	65.2%	38.9%	-	53.4	72.5	-	52.7%	12.4%	
18		165.0		112.9	68.4%	32.0%	-	71.0	101.1	-	59.0%	11.6%		
15		150.0		98.4	65.6%	42.9%	-	61.0	87.7	-	61.2%	12.2%		
10		100.0		82.7	82.7%	0.0%	80.8	52.7	66.4	2.3%	56.9%	24.5%		
17		180.0		92.8	51.5%	50.0%	-	53.4	90.4	-	73.6%	2.7%		
18		180.0		112.1	62.3%	50.0%	-	71.1	94.7	-	57.6%	18.4%		
18		175.0		101.3	57.9%	59.1%	-	61.6	87.9	-	64.5%	15.3%		
14		115.0		95.7	83.2%	9.5%	-	60.0	86.0	-	59.6%	11.3%		
12		140.0	113.2	80.9%	12.0%	-	76.5	99.0	-	48.0%	14.3%			
									Avg	2.3%	56.9%	24.5%		
50		14	145.0	132.3	91.2%	7.4%	-	82.6	103.6	-	60.2%	27.7%		
		14	125.0	103.6	82.9%	19.1%	-	65.9	99.5	-	57.2%	4.1%		
		18	165.0	139.8	84.7%	10.0%	-	88.1	111.6	-	58.6%	25.3%		
		15	150.0	122.9	81.9%	20.0%	-	74.8	101.2	-	64.3%	21.4%		
		10	100.0	96.2	96.2%	0.0%	84.4	69.2	85.9	13.9%	39.1%	12.0%		
		17	180.0	117.6	65.3%	44.0%	-	78.1	105.1	-	50.5%	11.9%		
		18	180.0	141.5	78.6%	24.1%	-	86.1	120.3	-	64.4%	17.6%		
	18	175.0	119.4	68.3%	25.0%	-	77.7	112.6	-	53.8%	6.1%			
	14	115.0	110.2	95.8%	0.0%	111.0	73.0	97.0	-0.7%	51.1%	13.6%			
12	140.0	136.2	97.3%	0.0%	115.1	93.7	105.4	18.3%	45.4%	29.2%				
									Avg	10.5%	45.2%	18.2%		
									Total Avg	3.0%	41.5%	19.9%		

Table 11: Extended results of DecQN compared with DAPP, RP, and GP on small instances

L	U	DecQN $_L$	DecQN	GLQ	GHQ	%DecQN	%GLQ	%GHQ	
S	L	765.6	799.7	738.3	834.0	-4.25%	3.71%	-8.19%	
	M	737.1	781.0	718.5	794.7	-5.62%	2.60%	-7.24%	
	H	722.4	751.0	704.9	760.4	-3.81%	2.48%	-5.00%	
M	L	1027.0	1054.8	1019.2	1077.5	-2.63%	0.77%	-4.69%	
	M	1017.7	1035.8	1002.8	1067.0	-1.75%	1.49%	-4.62%	
	H	1002.8	1023.8	977.1	1043.6	-2.06%	2.63%	-3.91%	
L	L	1079.0	1078.7	1078.3	1078.3	0.02%	0.06%	0.06%	
	M	1078.2	1080.3	1076.3	1076.9	-0.19%	0.18%	0.12%	
	H	1079.8	1081.4	1072.3	1075.3	-0.15%	0.70%	0.42%	
						Avg	-2.3%	1.6%	-3.7%

Table 12: Extended results of DecQN $_L$

L	U	DecQN $_U$	DecQN	GLQ	GHQ	%DecQN	%GLQ	%GHQ
S	L	773.5	799.7	738.3	834.0	-3.3%	4.8%	-7.2%
	M	760.2	781.0	718.5	794.7	-2.7%	5.8%	-4.3%
	H	745.3	751.0	704.9	760.4	-0.8%	5.7%	-2.0%
M	L	1051.7	1054.8	1019.2	1077.5	-0.3%	3.2%	-2.4%
	M	1038.6	1035.8	1002.8	1067.0	0.3%	3.6%	-2.7%
	H	1024.6	1023.8	977.1	1043.6	0.1%	4.9%	-1.8%
L	L	1078.7	1078.7	1078.3	1078.3	0.0%	0.0%	0.0%
	M	1080.3	1080.3	1076.3	1076.9	0.0%	0.4%	0.3%
	H	1080.3	1081.4	1072.3	1075.3	-0.1%	0.7%	0.5%
Avg						-0.7%	3.2%	-2.2%

Table 13: Extended results of DecQN $_U$

L	U	DecQN $_{All}$	DecQN	GLQ	GHQ	%DecQN	%GLQ	%GHQ
S	L	755.9	799.7	738.3	834.0	-5.5%	2.4%	-9.4%
	M	743.0	781.0	718.5	794.7	-4.9%	3.4%	-6.5%
	H	731.6	751.0	704.9	760.4	-2.6%	3.8%	-3.8%
M	L	1026.5	1054.8	1019.2	1077.5	-2.7%	0.7%	-4.7%
	M	1019.2	1035.8	1002.8	1067.0	-1.6%	1.6%	-4.5%
	H	1009.3	1023.8	977.1	1043.6	-1.4%	3.3%	-3.3%
L	L	1078.1	1078.7	1078.3	1078.3	-0.1%	0.0%	0.0%
	M	1078.7	1080.3	1076.3	1076.9	-0.1%	0.2%	0.2%
	H	1077.9	1081.4	1072.3	1075.3	-0.3%	0.5%	0.2%
Avg						-2.1%	1.8%	-3.5%

Table 14: Extended results of DecQN $_{All}$

action with the maximum Q value. This section investigates the use of the trained Q-network as a reward-to-go approximation function in an on-line RA. The approach presented in this experiment is similar to the solution method proposed in Ulmer et al. (2017), where an off-line trained value function is embedded into an RA in order to approximate the reward-to-go. In Section D.1, the proposed RA is explained in detail. We use instances and trained policies as illustrated in Section 6.1. Finally, we compare the performance of the proposed on-line-off-line DecQN with the purely off-line method in Section D.2.

D.1 Proposed Rollout Algorithm

The Rollout Algorithm is an on-line method in the form of forward-dynamic programming that can be viewed as a one-step policy iteration (Bertsekas 2013). Powell (2011) showed that if we roll out a known heuristic policy (the so-called base policy) to approximate reward-to-go values, the resulting policy will be improved over the base policy. In practice, the rollout algorithm estimates the reward-to-go value of an available action at the current decision epoch by simulating the base policy after choosing that action. Interested readers may refer to a survey by Bertsekas (2013) for a detailed discussion about RAs.

Similar to what defined in Equation (20), we let $V^\pi(s_k)$ be the expected reward that can be obtained by starting from the state s_k and following the base policy π . Accordingly, we define the rollout policy Π as:

$$\Pi(s_k) = \arg \max_{x_k \in A(s_k)} \left[R(s_k, x_k) + \mathbb{E}_{w \in W} [\gamma V^\pi(s_{k+1})] \right]. \quad (61)$$

In our case, the base policy is provided by the Q values trained by the DecQN method in the previous experiment. Therefore, we substitute the approximate value function $V^\pi(s_{k+1})$ according to Equation (32). Also, following the partially decentralized formulation, we replace s_k and $A(s_k)$ with $o_{k,\bar{v}}$ and $A(s_k, \bar{v})$, respectively. We rewrite the rollout policy Π as:

$$\Pi(o_{k,\bar{v}}) = \arg \max_{x_k \in A(s_k, \bar{v})} \left[R(o_{k,\bar{v}}, x_k) + \mathbb{E}_{w \in W} \left[\gamma \max_{x' \in A(s_{k+1}, \bar{v}')} Q(o_{k+1, \bar{v}'}, x') \right] \right], \quad (62)$$

where \bar{v}' represents the active vehicle in decision epoch $k + 1$.

Note that, since the set of customers is realized at the beginning of the operation, the customer demands are the only source of uncertainty in the equation above. Therefore, the expectation function $\mathbb{E}(\cdot)$ is computed

over a finite set of sample scenarios for the realization of the stochastic demands (W). It is important to note that, according to Equation (18), which defines the reward function for DecQN, the actual reward is realized with a delay. However, it is not feasible to wait to receive the actual reward through on-line methods, such as RA. Therefore, instead of using the reward function as in Equation (18), we define it as follows:

$$R(o_{k,\bar{v}}, x_k) = \begin{cases} \tilde{d}_c & x_k \text{ is a } c \in \mathcal{C}_0 \\ 0 & \text{otherwise} \end{cases}, \quad (63)$$

where \tilde{d}_c is the unserved demand of customer c , if its actual demand is already realized; otherwise, it is the expected demand.

The RA proceeds at decision epoch k by simulating the system for each possible action $x_k \in A(s_k, \bar{v})$ for one step and observe the immediate reward $R(o_{k,\bar{v}}, x_k)$ as well as the next observation $o_{k+1,\bar{v}'}$. In the next observation, the maximum Q value of available actions is considered as the approximate reward expected to be obtained onward, denoted as \bar{f} . The expected reward-to-go of each action is computed for a set of demand realizations (W). The action with the maximum \bar{f} will be selected as the best action to take (x^*) at decision epoch k .

Algorithm 4: Proposed Rollout Algorithm for decision epoch k

```

Initialize: set  $f^*$  to 0
Construct the action space  $A(s_k, \bar{v})$ 
for  $x_k \in A(s_k, \bar{v})$  do
     $\bar{f} \leftarrow 0$ 
     $o_{k,\bar{v}} \leftarrow O(s_k, \bar{v})$ 
    Take action  $x_k$  and receive the reward  $r_k = R(o_{k,\bar{v}}, x_k)$ 
    for  $w \in W$  do
        State transition  $k$  to  $k + 1$ :
         $s_{k+1} \leftarrow S^M(s_k, x_k, w)$ 
         $\bar{v}' \leftarrow \{v \in \mathcal{V} | a_v = \min_{v \in \mathcal{V}} a_v\}$ 
         $o_{k+1,\bar{v}'} \leftarrow O(s_{k+1}, \bar{v}')$ 
        Take action  $x_{k+1} = \arg \max_{x'} Q(o_{k+1,\bar{v}'}, x')$  and receive  $r'_k = R(o_{k+1,\bar{v}'}, x_{k+1})$ 
        state transition  $k + 1$  to  $k + 2$ :
         $s_{k+2} \leftarrow S^M(s_{k+1}, x_{k+1}, w)$ 
         $\bar{v}'' \leftarrow \{v \in \mathcal{V} | a_v = \min_{v \in \mathcal{V}} a_v\}$ 
         $o_{k+2,\bar{v}''} \leftarrow O(s_{k+2}, \bar{v}'')$ 
         $f \leftarrow [r_k + \gamma r'_k + \gamma^2 \max_{x_{k+2} \in A(s_{k+2}, \bar{v}'')} Q(o_{k+2,\bar{v}'}, x_{k+2})]$ 
         $\bar{f} \leftarrow \bar{f} + f$ 
    end
     $\bar{f} \leftarrow \bar{f} / |W|$ 
    if  $\bar{f} > f^*$  then
         $x^* \leftarrow x_k$ 
         $f^* \leftarrow \bar{f}$ 
    end
end
return  $x^*$ 

```

Given the delayed reward mechanism, we decided to simulate the problem for two steps for each action (instead of the traditional one-step) in our implementation. Therefore, the implemented Equation (62) has been modified as:

$$\Pi(o_{k,\bar{v}}) = \arg \max_{x_k \in A(s_k, \bar{v})} \mathbb{E} [R(o_{k,\bar{v}}, x_k) + \gamma R(o_{k+1,\bar{v}'}, x_{k+1}) + \gamma^2 \max_{x_{k+2} \in A(s_{k+2}, \bar{v}'')} Q(o_{k+2,\bar{v}'}, x_{k+2})], \quad (64)$$

where x_{k+1} is the action in decision epoch $k+1$ according to the base policy π (i.e., $x_{k+1} = \arg \max_{x' \in A(s_{k+1}, \bar{v}')} Q(o_{k+1,\bar{v}'}, x')$) and \bar{v}'' is the active vehicle in decision epoch $k + 2$. Algorithm 4 illustrates our proposed RA for each decision epoch k , when the active vehicle is \bar{v} , the global state is s_k , and W is a finite set of demand realizations.

D.2 Results and Discussion

In Section 6.1, we tested each trained policy for 250,000 realizations. However, because the rollout algorithm requires substantial on-line computing, testing across the same realization set would be computationally expensive. Therefore, we test the proposed on-line-off-line DecQN for each instance $i \in I$, with $I = \mathcal{D} \times \mathcal{Q}$, on $\tilde{I}(i)$ with 2,500 realizations (50 customer realizations \times 50 demand realizations). Furthermore, we only focus on harder instances with $\mathcal{D} = \{\text{Moderate, High, Very High}\}$. For this experiment, we set the size of the sample scenarios for the rollout algorithm ($|W|$) to 50. Table 15 reports the results of the on-line-off-line

Ψ_{n_z}	Q	RA-DecQN	DecQN	%DecQN
Moderate	25	164.3	161.3	1.9%
	50	202.7	196.9	3.0%
	75	217.1	211.9	2.5%
High	25	358.3	358.2	0.0%
	50	461.0	455.4	1.2%
	75	510.5	501.5	1.8%
Very High	25	551.7	551.7	0.0%
	50	708.7	701.4	1.0%
	75	790.3	776.7	1.8%
Avg				1.5%

Table 15: Results of on-line-off-line DecQN compared with off-line DecQN

DecQN (RA-DecQN) and compares them with the performance of the off-line policy (DecQN). The average improvement of the rollout algorithm over the off-line DecQN is seen in column %DecQN. According to the results, the proposed rollout outperforms the off-line version by an average of 1.5% in all cases. The average improvement of the rollout algorithm over the off-line DecQN is shown in Table 16. This table helps us to analyze how changes in customer density and vehicle capacity affect %DecQN. Accordingly, as the customer density decreases from Very High to Moderate, the gap widens significantly. Specifically, the average improvement over the off-line DecQN in instances with Very High customer density is 0.9%, whereas this value in instances with Moderate density is 2.4%. It is essential to notice that, as discussed in Section 6.1, the importance of a good routing strategy is magnified in instances with a lower customer density. This finding shows that the on-line-off-line method improves the off-line policy in terms of routing aspects. Furthermore, the sensitivity analysis over the changes in the vehicle capacity also confirms this finding. According to Table 16, the improvement percentage considerably increases from 0.6% to 2.0% when the vehicle capacity changes from 25 to 75. It is worth to notice that as the vehicle capacity becomes larger, vehicles are allowed to perform longer routes which highlights the necessity of an effective routing strategy. In Section 6.1, we demonstrated that the average improvement over GP drops from 11.2% to 7.9%, when

%DecQN	Q			Avg
	25	50	75	
Moderate	1.9%	3.0%	2.5%	2.4%
High	0.0%	1.2%	1.8%	1.0%
Very High	0.0%	1.0%	1.8%	0.9%
Avg	0.6%	1.7%	2.0%	1.5%

Table 16: Average improvement of on-line-off-line DecQN over off-line DecQN

the vehicle capacity increases from 25 to 75. However, this experiment shows that the on-line-off-line DecQN partly compensates for this reduction.

In this experiment, the average computing time per decision epoch for Moderate, High, and Very High customer density is 0.10, 0.17, and 0.21 seconds, respectively. Although, as expected, the computation time grows as the number of customers increases, the on-line-off-line DecQN can decide in 0.21 seconds, even in the most complex problems. Therefore, the proposed rollout algorithm can also be regarded as an efficient on-line method.

References

- Powell WB, 2011 *Approximate dynamic programming*. Wiley Series in Probability and Statistics (Hoboken, NJ, USA: John Wiley & Sons, Inc.).
- Gendreau M, Laporte G, Séguin R, 1995 *An exact algorithm for the vehicle routing problem with stochastic demands and customers*. *Transportation Science* 29(2):143–155.
- Goodson JC, Ohlmann JW, Thomas BW, 2013 *Rollout policies for dynamic solutions to the multivehicle routing problem with stochastic demand and duration limits*. *Operations Research* 61(1):138–154.
- Goodson JC, Thomas BW, Ohlmann JW, 2016 *Restocking-based rollout policies for the vehicle routing problem with stochastic demand and duration limits*. *Transportation Science* 50(2):591–607.
- Solomon MM, 1987 *Algorithms for the vehicle routing and scheduling problems with time window constraints*. *Operations Research* 35(2):254–265.
- Kullman ND, Cousineau M, Goodson JC, et al., 2021 *Dynamic ride-hailing with electric vehicles*. *Transportation Science* In press.
- Ulmer MW, Goodson JC, Mattfeld DC, et al., 2017 *Offline-online approximate dynamic programming for dynamic vehicle routing with stochastic requests*. *Transportation Science* 53(1):1–35.
- Bertsekas DP, 2013 *Rollout algorithms for discrete optimization: A survey*. Pardalos PM, Du DZ, Graham RL, eds., *Handbook of Combinatorial Optimization*, 2989–3013 (New York, NY: Springer New York).